CAPITAL UNIVERSITY OF SCIENCE AND TECHNOLOGY, ISLAMABAD

Magneto-micropolar nanofluid flow over a convectively heated sheet with non-linear radiation and viscous dissipation

by

Abid Hussain

A thesis submitted in partial fulfillment for the degree of M. Phil Mathematics

in the

Faculty of Computing
Department of Mathematics

2018

CAPITAL UNIVERSITY OF SCIENCE & TECHNOLOGY
ISLAMABAD

CERTIFICATE OF APPROVAL

Magneto-micropolar nanofluid flow over a convectively heated sheet with non-linear radiation and viscous dissipation

by

Abid Hussain
MMT153012

THESIS EXAMINING COMMITTEE

S. No.	Examiner	Name	Organization
(a)	External Examiner	Dr. Rashid Mahmood	AIR University Islamabad
(b)	Internal Examiner	Dr. Shafqat Hussain	CUST Islamabad
(c)	Supervisor	Dr. Muhammad Sagheer	CUST Islamabad

Thesis Supervisor
Dr. Muhammad Sagheer
May, 2018

Dr. Muhammad Sagheer
Head
Dept. of Mathematics
May, 2018

Dr. Muhammad Abdul Qadir
Dean
Faculty of Computing
May, 2018

Author's Declaration

I, **Abid Hussain** hereby state that my M. Phil thesis titled "**Magneto-micropolar nanofluid flow over a convectively heated sheet with non-linear radiation and viscous dissipation**" is my own work and has not been submitted previously by me for taking any degree from Capital University of Science and Technology, Islamabad or anywhere else in the country/abroad.

At any time if my statement is found to be incorrect even after my graduation, the University has the right to withdraw my M. Phil Degree.

(Abid Hussain)

Registration No: MMT153012

Plagiarism Undertaking

I solemnly declare that research work presented in this thesis titled "*Magneto-micropolar nanofluid flow over a convectively heated sheet with non-linear radiation and viscous dissipation*" is solely my research work with no significant contribution from any other person. Small contribution/help wherever taken has been dully acknowledged and that complete thesis has been written by me.

I understand the zero tolerance policy of the HEC and Capital University of Science and Technology towards plagiarism. Therefore, I as an author of the above titled thesis declare that no portion of my thesis has been plagiarized and any material used as reference is properly referred/cited.

I undertake that if I am found guilty of any formal plagiarism in the above titled thesis even after award of M. Phil Degree, the University reserves the right to withdraw/revoke my M. Phil degree and that HEC and the University have the right to publish my name on the HEC/University website on which names of students are placed who submitted plagiarized work.

(Abid Hussain)

Registration No: MMT153012

Acknowledgements

First and foremost I would like to pay my cordial gratitude to the Almighty **Allah**, Who created us as a human being with the great boon of intellect. I would like to pay my humble gratitude to the Allah Almighty, for blessing us with the Holy Prophet **Hazrat Muhammad (Sallallahu Alaihay Wa'alihi wasalam)** for whom the whole universe is being created. He (Sallallahu Alaihay Wa'alihi wasalam) removed the ignorance from the society and brought us out of darkness. Thanks again to that Monorealistic Power for granting me with a strength and courage whereby I dedicately completed my MPhil thesis with positive and significant result.

I owe honour, reverence and indebtedness to my accomplished supervisor and mentor **Dr. MUHAMMAD SAGHEER** whose affectionate guidance, authentic supervision, keen interest and ingenuity was a source of inspiration for commencement, advancement and completion of the present study. I would like to acknowledge CUST to providing me such a favourable environment to conduct this research. My especial thanks to **Muhammad Bilal**, for his inspiring guidance and untiring help during the research period.

Thanks to my fiancee **Ayesha Khizar** for her ever encouragement and overall support during my entire university life.

It will be injustice if I forget my beloved parents, brothers, sisters and kind persons. Thanks to my father **Sakhi Muhammad**, my great mother **Khatam Jan**, brothers **Muhammad farooq**, **Gulfraz**, **Tariq**, and **Habib**, and my dear sisters **Azmat**, and **Maryam**, for their ever encouragement and overall support during my entire university life. May Almighty Allah shower his blessings and prosperity on all those who assisted me during the completion of this thesis.

Abstract

A mathematical model is presented for analyzing the flow of magneto-micropolar nanofluid above a convectively heated permeable stretching sheet with non-linear radiation and viscous dissipation. The similarity transformation is utilized to change the governing partial differential equations (PDEs) to the system of non-linear ordinary differential equations (ODEs). The resulting system of ODEs is sorted out mathematically by utilizing the shooting method and the obtained mathematical outcomes are compared with those obtained using the MATLAB built-in function bvp4c. Numerical values of the physical quantities like, the skin friction coefficient, the Sherwood number and the Nusselt number for the emerging parameters such as, Pr, Nb, Nt, and Le, etc, are also computed and discussed in this work.

Contents

List of Figures

List of Tables

Nomenclature

a	dimensional constant
Pr	Prandtl number
B_0	magnetic field strength
q_m	surface heat flux
C	nanoparticles concentration
q_r	radiative heat flux
C_f	concentration at wall
q_w	surface mass flux
C_∞	ambient concentration
R	radiation parameter
C_p	specific heat
Re	Reynolds number
C_{fx}	skin friction in $x-$direction
Sh_x	Sherwood number
D_B	coefficient of Brownian diffusion
T	fluid temperature
D_T	coefficient for thermophoresis diffusion
T_f	hot fluid temperature
E	electric parameter
T_∞	ambient temperature
E_0	applied electric field
(u, v)	velocity vectors
Ec	Eckert number
(x, y)	axial and normal coordinates

f	dimensional velocity component
α	slip parameter
f_w	suction/injection velocity
α^*	slip coefficient
Gr	Grashof number
γ^*	spin gradient viscosity
G	micro-rotation or angular velocity
γ_1	thermal Biot number
h	dimensionless transverse velocity
γ_2	solutal Biot number
h_f	heat flux coefficient
η	dimensionless normal distance
j	micro inertia density
θ	dimensionless temperature
k	vortex viscosity
μ	dynamic viscosity
K	material parameter
ν	kinematic viscosity
k_1	thermal conductivity
ρ	fluid density
Le	Lewis number
σ	electric conductivity
M	magnetic parameter
τ	ratio of heat capacities
Nb	Brownian motion parameter
τ_{wx}	wall shear stress in x-direction
Nt	thermophoresis parameter
ϕ	dimensionless concentration
Nu_x	Nusselt number

Chapter 1

Introduction

The science which analyzes the movement of a highly conducting fluid within the presence of a magnetic field is termed as the Magnetohydrodynamics (MHD). Analysis of Newtonian and non-Newtonian flows in the presence of magnetic field has innumerable applications in industries and engineering. Some prominent uses of MHD can be seen in the cooling system with fluid metals, MHD power generators, liquid beads and sprays, accelerators, atomic reactors, preparing of nourishment stuffs, oil industry, microelectronic gadgets, geothermal energy extractions of metals and so on. Ahmad et al. [1] investigated the semi-inverse solutions for nonuniform magnetohydrodynamic stream of second-grade fluid over stretching surface. Irregular magnetohydrodynamic mixed convection stream of second-grade nano-fluid induced by stretching plane with thermal radiation was observed by Ramzan and Bilal [2]. Ellahi [3] examined the magnetohydrodynamic flow of non-ideal nano-fluid in a tube. Govindaraju et al. [4] studied the entropy modeling of the nanofluid and MHD flow over a nonlinear stretching surface. MHD rotating flow of water based nano-fluids moving in parallel plates was discussed by Sheikholeslami et al. [5]. Lin et al. [6] examined the heat transfer impacts on MHD flow of pseudo-plastic fluid loaded with antiparticles. Hayat et al. [7] analyzed the three dimensional MHD stream of Maxwell nano-fluid through convective boundary. Ahmad and Asghar [8] inspected the magnetohydrodynamic flow of second-grade fluid above the stretching plane. Hayat et al. [9] analyzed

the magnetohydrodynamic (MHD) flow of second-grade nanofluid because of a nonlinear stretching surface. Ariel [10] also examined the computational aspects for MHD stream close to a pivoting disk. Numerous comparative investigations are contemplating the significance of fluid movement through various physical phenomenon can be seen in [11–13].

The impact of thermal rays is essential in space technology and high temperature processes. At the point when the temperature variation is very high, the linear thermal radiation causes a noticeable error. To overcome such errors, nonlinear thermal radiation is taken into account. The impact of chemical reaction and thermal radiation on the flow over stretching surface with outer heat source was explained by Krishna et al. [14]. Researchers and scientists have done a series of research work to highlight the importance of thermal radiation [15–17].

Mixed convection is one of the transport phenomena which is composed of both natural and forced convection flow. Mixed convection flow, appear in many transport processes both naturally and in engineering applications. Industrial and technical processes incorporating the solar central receivers exposed to winds, electronic gadgets cooled by fans and nuclear reactors cooled in case of emergence shutdown. Abo-Eldahab et al. [18] examined the magneto-hydrodynamic free heat transfer flow past a semi-infinite vertical strip with mass exchange and Hall effects. Mixed convection boundary layer is influenced by Hall current and Ohmic heating. Impacts on flow of a micropolar fluid from a circular cone with power-law fluid at stretching surface was studied by Abo-Eldahab et al. [19]. The impact of Hall current and chemical reaction on hydromagnetic flow of a vertical stretching plane with interior heat absorption was presented by Salem and El-Aziz [20].

Micropolar fluids are those which contain micro-constituents that can undergo rotation, the appearance of which can influence the hydrodynamics of the stream so that it can be clearly non-Newtonian. Different types of non-ideal fluids can be seen in routine life such as, macromolecules, animal blood, and shampoo, etc.

Eringen's [21] pioneering work in micropoler fluids opened the entryways in non-ideal fluids. Nadeem et al. [22] explored the affects of hydrodynamic flow of micropaler nano-fluid between parallel plates in a rotating procedure. Impact of radiation transfer and chemical reactions on micropoler fluid flow with perforated wells forming a path is given by Fakoura et al. [23]. Hayat et al. [24] considered the micropoler fluid flow affected by chemical reaction and thermal radiation.

Nanoparticles in different base fluids can alter the fluid stream and heat transfer. These suspensions of micro particles in the fluids are called nano-fluids. Nano-fluids have received a prominent attention because of their huge spectrum of applications in atomic reactors, transportation, food, microbial fuel cell technology, polymer covering, intelligent building design, micro fluid conveyance gadgets and aerospace trilogy. Choi [25] presented the term nanofluid and depicted that the heat characteristics of the fluids are increased when we incorporate the nanoparticles in fluids. Boundary-layer flow of nano-fluid above linear stretching plane exposed to the convective boundary condition was analyzed by Makinde and Aziz [26]. Lin et al. [27] highlighted the usefulness of the magnetic lines of force in time-directive movement of pseudo-plastic fluid above a thin layer by taking in to account the inner radiation source impact. Free-convective flow of magnetic dependent velocity nano-fluid was given by Sheikholeslami et al. [28]. Khan and Pop [29] analyzed the nanofluid flow bounded by a stretchable surface using numerical approach. They concluded that Brownian motion and thermophoresis effects enhance the penetration depth of heat. Pal et al. [30] examined the impacts of magnetic lines of force on radiation transfer above a non-linear expanding plate in nano-fluid with thermal radiation. Rashidi et al. [31] examined the magneto-hydradynamic flow of nano-fluid by a rotating perforated disk with disorderness. Sheikholeslami et al. [32] described the radiation transform studies of nano-fluid equipped with perforated medium past a porous stretching boundary. More related research involving nanofluids can be seen through the investigations [33–35].

Thesis contribution:

In this thesis, we provide a review study of Ramzan et al. [36] and extend the flow analysis by considering the additional effects of Nanofluid, viscous dissipation and non linear thermal radiation with the assumptions of laminar, steady, incompressible, two dimensional, porous stretching sheet, Joule heating, micropolar nanofluid with elector-hydrodynamic, convective boundary condition and micro-slip condition on the wall. The obtained system of PDEs is transformed into a system of non-liner and coupled ODEs by using a suitable similarity transformation. A numerical solution of the system of ODEs is obtained by employing the shooting method and the precision of the obtained numerical results is compared by using the Matlab bvp4c function. The mathematical inferences are discussed for different physical parameters appearing in the solution influencing the flow and heat transform.

Thesis outline:

The thesis is compiled as:

Chapter 2 includes the fundamental definitions and terminologies used throughout the thesis.

Chapter 3 contains a comprehensive numerical review of [36]. A numerical study of micropolar, partial slip, MHD flow with convective boundary condition is analyzed. The constitutive of the flow model expression are sorted out numerically and the impact of physical parameters concerning the flow model on dimensionless energy, velocity, and microrotation are presented through graphs and tables. A comparison of the achieved numerical results with the published results of Ramzan et al. [36] is also presented.

In **Chapter 4**, we discuss the partial slip effects on magneto-micropolar nanofluid movement and heat exchange past a convectively heated sheet with nonlinear thermal radiation and viscous dissipation. The reduced system of ODEs after applying a proper similarity transform is solved numerically. Graphs and tables describe the behavior of physical quantities such as, Pr, Nb, Nt, and Le etc. Numerical values of skin friction coefficient, Sherwood number and Nuselt number have also been computed and discussed in this Chapter.

In **Chapter 5**, major conclusion are drawn through the summary of the dissertation.

All the references used in this dissertation are listed in **Bibliography**.

Chapter 2

Basic definitions and governing equations

In this chapter, some basic laws, concepts, terminologies and definitions will be explained, which will be helpful in the next chapters.

2.1 Fluid

In mathematical literature, the material which alters continuously by the effect of shear stress is called a fluid. It doesn't matter what kind of shear stress it is. The shape of the fluid is also changed through the act of shear stress. Liquids and Gases are the examples of fluid.

2.1.1 Fluid Mechanics

The area of physical sciences that studies the action of fluid in static or dynamic condition is called the fluid mechanics. It has further categories presented below.

2.1.2 Fluid Statics

A branch of fluid mechanics that deals with the fluid and its characteristics at a fixed position, is called the fluid statics.

2.1.3 Fluid dynamics [37]

"The study of application of laws of forces and motion on the moving fluid is given the name of fluid dynamics. The main principle which deals this motion, is the Newtons second law of motion i.e., $F = ma$, where F is applied force, m is mass of body and a is acceleration of body due to applied force."

2.2 Uniform and non-uniform flow [37]

"If the magnitude and direction of stream velocity is the same at each point in the fluid, it is known as the uniform flow. But if the velocity is not the same at each point of the flow, at a given instant, then the flow become non-uniform."

2.3 Steady flow [37]

"Steady flow is defined as that type of flow in which the physical properties of the fluid like velocity, pressure, density, etc., at a specific point do not change with time. Let λ be any fluid property, then the following holds for the steady flow.

$$\frac{\partial \lambda}{\partial t} = 0,$$

where λ is any fluid property."

2.4 Unsteady flow [37]

"If any physical property of the fluid at a specific point changes with time then such flow is called the unsteady flow. Let λ be any fluid property, then the following holds for an unsteady flow."

$$\frac{\partial \lambda}{\partial t} \neq 0.$$

2.5 Laminar and turbulent flows [38]

"A laminar flow is one in which the fluid particles move in smooth layers, or laminas. In such flow, the path lines of fluid particles do not intersect each other. A turbulent is one in which the fluid particles rapidly mix as they move along due to random three dimensional velocity fluctuations. i.e., fluid particles change directions continuously, is called the turbulent flow."

2.6 Compressible and incompressible flow [38]

"The flow type in which the density is constant within the fluid, is called an incompressible flow. The mathematical equation for an incompressible flow is given by

$$\frac{D\rho}{Dt} = 0,$$

where ρ denotes the fluid density and $\frac{D}{Dt}$ is the material derivative given by

$$\frac{D}{Dt} = \frac{\partial}{\partial t} + \mathbf{V} \cdot \nabla. \tag{2.1}$$

In Eq. (2.1), $\mathbf{V}$ denotes the velocity of the flow and ∇ is the differential operator. In Cartesian coordinate system ∇ is given as

$$\nabla = \frac{\partial}{\partial x}\hat{i} + \frac{\partial}{\partial y}\hat{j} + \frac{\partial}{\partial z}\hat{k}.$$

The fluid flow in which the density variation is not negligible, is termed as a compressible flow."

2.7 Viscosity [38]

"Viscosity is an intrinsic property of the fluid that measures the fluid's resistance. In other words, it is a measure of how much force is required to move from one layer of the fluid to another layer. Usually liquids and gases have non-zero viscosity. The coefficient of viscosity is denoted by the symbol μ. Viscosity can be described in the following two different ways."

2.7.1 Dynamic viscosity [37]

"It is defined as the resistance offered to a layers of the fluid, when it moves over another layer of the fluid. When two layer of a fluid, a distance by apart, move over the other with different velocities, then the viscosity together with relative velocity cause a shear stress acting between the fluid layers. This shear stress is proportional to the rate of change of velocity with respect to the velocity gradient. Mathematically, it can be written as:

$$\text{Viscosity}(\mu) = \frac{\text{Shear stress}}{\text{Rate of shear strain}}.$$

In the above expression, μ is the coefficient of viscosity. This is also known as the absolute viscosity or the dynamic viscosity having dimension $[ML^{-1}T^{-1}]$. Unit of viscosity in SI system is kg/ms or Pascal-second [Pa.s]."

2.7.2 Kinematic Viscosity [37]

"The kinematic viscosity depicts the ratio of the dynamic viscosity μ to the density of the fluid ρ. It is represented by ν. Mathematically,

$$\nu = \frac{\mu}{\rho}.$$

The dimension of kinematic viscosity is $[L^2T^{-1}]$ and its unit in SI system is m^2/s."

2.8 Newtonian and non-Newtonian fluid [37]

"The real fluids, in which the the shear stress is directly proportional to the rate of shear strain (or velocity gradient), are known as the Newtonian fluids. Their behavior is given by the relation

$$\tau = \mu \frac{du}{dy}.$$

In the above equation, τ is the stress tensor, μ is the viscosity and $\frac{du}{dy}$ is the deformation rate. The real fluids, in which the the shear stress is not proportional to the rate of shear strain (or velocity gradient), are known as the non-Newtonian fluids."

2.9 Generalized continuity equation [39]

"The continuity equation implies a balance between the masses entering and leaving a control volume per unit time and the change in density within it. For the unsteady flow of a compressible fluid, the conservation of mass applied to a fluid passing through an infinitesimal, fixed control volume yields the following equation of continuity:

$$\frac{\partial \rho}{\partial t} + \nabla.(\rho \mathbf{V}) = 0. \tag{2.2}$$

The first term in this equation represents the rate of increase of density in the control volume and the second term represents the rate of mass flux passing out of the control surface per unit volume. If the fluid is incompressible, then Eq. (2.2) reduces to

$$\nabla \cdot \mathbf{V} = 0.$$

Above relation holds for a steady or an unsteady incompressible flow."

2.10 Generalized momentum equation [39]

"The momentum equation is derived from Newton's law of motion. Further, in fluid motion it is necessary to consider two types of forces separately, (1) forces acting throughout the mass of the fluid element, known as body forces, and (2) forces acting on the boundary, known as surface forces. F is denoting the sum of above two types of forces, then the momentum equation can be written as

$$m\frac{D\mathbf{V}}{Dt} = \mathbf{F}.$$

The flow of the fluid is represented by the differential equation as

$$\rho\frac{D\mathbf{V}}{Dt} = \nabla.\tau + \rho\mathbf{b},$$

where $\rho\mathbf{b}$ is the net body force, $\nabla.\tau$ the surface force and τ the Cauchy stress tensor."

2.11 Magnetohydrodynamics [38]

"The magnetohydrodynamics is a combination of three words. Magneto means the magnetic field, hydro stands for water and dynamics for the movement. The study of the motion of electrically conducting fluids in which current is induced

by the magnetic field, is known as the magnetohydrodynamics (MHD). Examples of such fluids are plasmas, electrolytes, salt water and liquid metals."

2.12 Porosity [40]

"The porosity is the ratio of volume of pores to the bulk volume of a porous medium. A porous medium is often identified by its porosity. The momentum equation with porosity and MHD, is as follows.

$$\rho\frac{D\mathbf{V}}{Dt} = \nabla.\tau - \rho\sigma\mathbf{B^2V} - \rho k\mathbf{V}. \tag{2.3}$$

Here, k and $\mathbf{B}$ are the porosity and magnetic field of the medium respectively."

2.13 Heat transfer [40]

"Heat transfer is the energy transfer due to temperature difference. When there is a temperature difference in a medium or between media, heat transfer must take place. Heat transfer can occur through the following three mechanisms."

2.14 Conduction

The way in which the transfer of heat phenomenon occurs, due to physical contact of the bodies or the systems, is called conduction. Ironing clothes, melting piece of ice in hand and becoming hot, the bonnet or hood of a car, metal spoon in boiling water, a cup with hot coffee, all are the examples of conduction.

2.15 Convection [40]

"Convection is the transfer of heat through fluids (gases or liquids) from a warmer place to a cooler place. In fluid dynamics, convection is the energy transfer due to bulk fluid motion. Convective heat transfer arises between a fluid in motion and a bounding surface. If there is a difference in the temperature of the fluid and the bounding surface, then the thermal boundary layer is created. Fluid particles which interact with the surface, attain equilibrium at the surface temperature and transfer energy in the next layer and so on. Through this mode, temperature gradients are produced in the fluid. The area of fluid containing these temperature gradients identified as the thermal boundary layer. Since the convective heat transfer is by both the random molecular motion and the bulk motion of the fluid, the molecular motion is more adjacent to the surface where the fluid velocity is less. Convective heat transfer depends upon the nature of the flow. Therefore convection has three forms: Forced convection, Natural (free) convection, and Mixed convection."

2.15.1 Forced convection [40]

"Forced convection is a process, or kind of energy transfer in which fluid motion is produced by an external source. It is be deliberated as one of the core techniques of useful heat transfer as a weighted amount of heat energy can be transferred very efficiently. In other words, a technique of heat transfer in which fluid motion is originated by an independent source like a pump and fan etc., is called the forced convection."

2.15.2 Natural convection [40]

"Natural convection is a heat transport process, in which the fluid motion is not developed by any external source, but only by the density differences in the fluid

taking place due to the temperature gradients. It happens due to the temperature differences which affect the density of the fluid. It is also known as free convection."

2.15.3 Mixed convection [40]

"It is a combination of both the forced convection and the natural convection and occurs when natural convection and forced convection act collectively to transfer the heat."

2.16 Radiation [40]

"Radiation is the energy transfer due to release/discharge of the electromagnetic waves or photons from a surface volume. Radiation doesn't require any medium to transfer heat. The energy produced by radiation is transformed by the electromagnetic waves."

2.17 Thermal conductivity [40]

"The property of a material to pass on heat through it by conduction, is known as the thermal conductivity. Mathematically it is given by the relation

$$\kappa = \frac{q\nabla l}{S\nabla T},$$

where q is the heat passing through a surface area S and causing a temperature difference ∇T over a distance of ∇l. Here l, S and ∇T all are assumed to be of unit measurement. The unit of thermal conductivity in SI system is $\frac{W}{m.\kappa}$ and its dimension is $[MLT^{-3}\theta^{-1}]$."

2.18 Thermal diffusivity [37]

"Thermal diffusivity is a material property for characterizing unsteady heat conduction. Mathematically, it can be expressed as

$$\alpha = \frac{\kappa}{\rho C_p},$$

where κ, ρ and C_p represent the thermal conductivity of material, the density and the specific heat capacity of material respectively . The unit and dimension of thermal diffusivity in SI system are $m^2 s^{-1}$ and $[LT^{-1}]$ respectively."

2.19 Dimensionless numbers

2.19.1 Reynolds number [37]

"It is the most significant dimensionless number which is used to identify the different flow behaviors like laminar or turbulent flow. It helps to measure the ratio between the inertial force and the viscous force. Mathematically,

$$Re = \frac{\frac{\rho U^2}{L}}{\frac{\mu U}{L^2}} \quad \Longrightarrow \quad Re = \frac{LU}{\nu},$$

where U denotes the free stream velocity, L the characteristics length and ν stands for the kinematic viscosity. At low Reynolds number, laminar flow arises, where the viscous forces are dominant. At high Reynolds number, turbulent flow arises, where the inertial forces are dominant."

2.19.2 Prandtl number [37]

"It is the ratio between the momentum diffusivity (ν) and the thermal diffusivity (α). Mathematically, it can be written as,

$$Pr = \frac{\nu}{\alpha} \implies \frac{\mu/\rho}{k/C_p\rho} \implies \frac{\mu c_p}{k},$$

where μ represents the dynamic viscosity, C_p denotes the specific heat and κ stands for the thermal conductivity. The relative thickness of thermal and momentum boundary layer controlled by Prandtl number. For small Pr, the thermal boundary layer becomes thicker than the velocity boundary layer."

2.19.3 Nusselt number [37]

"The Nusselt number is the ratio of the convective to the conductive heat transfer across (normal to) the boundary. Mathematically, it can be written as:

$$Nu = \frac{hL}{\kappa},$$

where h stands for the convective heat transfer, L for the characteristics length and κ for the thermal conductivity."

2.19.4 Skin friction coefficient [37]

"The skin friction coefficient occurs due to the friction between the fluid and the solid surface which leads to slow down the motion of the fluid. The skin friction coefficient can be defined as,

$$C_f = \frac{2\tau_w}{\rho U^2},$$

where τ_w denotes the wall shear stress, ρ the density and U the free-stream velocity."

2.19.5 Darcy's number

Henry Darcy (1856) is the mathematician who introduced this number and non dimensionalising the of Darcy's law was its cause. The Darcy's number is the representative of the relevant effects of the permeability of the medium compared with its cross - sectional area. Mathematically,

$$D_a = \frac{\kappa}{a^2},$$

where a is the diameter of the particle and κ shows the porosity.

2.20 Boundary layer flow [38]

"A layer of reduced velocity in the fluid is called the boundary layer. It is exactly adjacent to the solid surface which is just following the fluid. The basic idea of boundary layer in motion of a fluid over a surface was first introduced by Ludwig Prandtl (1874-1953). All the work done further in the fields of separation, heat transfer and skin friction was due to the basic idea and knowledge given by him in his papers. The reason why we have the velocity zero, exactly adjacent to the layer, is that the viscous effect and the layer of the fluid which is making contact with the surface becomes slowly adhered to the surface resulting in a condition of no-slip. The phenomenon of shearing takes place in the process due to the fact that the layers of the fluid are moving. The shear acting between two walls and the layer just next to it is called the wall shear and is denoted by T_w. The ratio of two important forces determined by the Reynolds number plays an important role in determination of the thickness of the boundary layer. When the Reynolds number has a low value, the denominator of it in other words the viscous forces dominate and have more effect and in result the flow is laminar and for vice versa, the inertial forces dominate and they result in the turbulent flow". There are two types of the boundary layer.

- Hydrodynamic (velocity) boundary layer

- Thermal boundary layer

2.20.1 Hydrodynamic boundary layer

"A region of the fluid flow where the transition from zero velocity at the solid surface to the free stream velocity at some extent far from the surface in the direction normal to the flow takes place in a very thin layer, is known as the hydrodynamic boundary layer."

2.20.2 Thermal boundary layer [38]

"The heat transfer exchange surface and the free stream have a liquid or a gaseous agent for heat transfer. From wall to free stream, we come across the change of temperature of heat transfer agent. It increases from wall to the main stream. The surface temperature is assumed to be equal to the temperature of the fluid layer close to the wall inside the boundary and this temperature is equal to the temperature of the bulk at some point in the fluid."

2.20.3 Concentration boundary layer [38]

"The concentration boundary layer develops when there is a difference in concentration of a component between the free stream and the surface. A concentration profile develops, and the thickness of the concentration boundary layer is defined as that point at which the difference in concentration between the fluid and the surface is 99 percent of the difference in concentration between the free stream fluid and the surface."

2.21 Viscous dissipation [40]

"The viscous dissipation is the destruction of fluctuating velocity gradients by the action of viscous stresses."

2.22 Micropolar fluid [38]

"Micropolar fluids are fluids with micro structure. They belong to a class of fluids with non symmetric stress tensor that we shall call the polar fluids, and include, as a special case, the well-established Navier-Stokes model of classical fluids that we shall call ordinary fluids. Physically, micropolar fluids may represent fluids consisting of rigid, randomly oriented (or spherical) particles suspended in a viscous medium, where the deformation of fluid particles is ignored."

2.23 Nanofluid

A nanofluid is a conventional fluid containing the nanometer-sized particles.

Chapter 3

Radiative and Joule heating effects in the MHD flow of a micropolar fluid with partial slip and convective boundary condition

3.1 Introduction

In this chapter, the numerical study of the flow of micropoler fluid above a porous stretching sheet in the presence of Joule heating, thermal radiation, flow on an unsteady stretching surface and Magnetohydrodynamic with heat transfer through moving fluid [36] is discuses. A proper similarity transformation is utilized to convert the boundary layer equations into the nonlinear and coupled ordinary differential equations. These ODEs are sorted out numerically by applying the shooting mechanism. Graphical representations are also included to explain the effect of evolving parameters against the above mentioned distributions. Finally, the numerical outcomes are discussed at the end of the chapter.

3.2 Problem Formulation

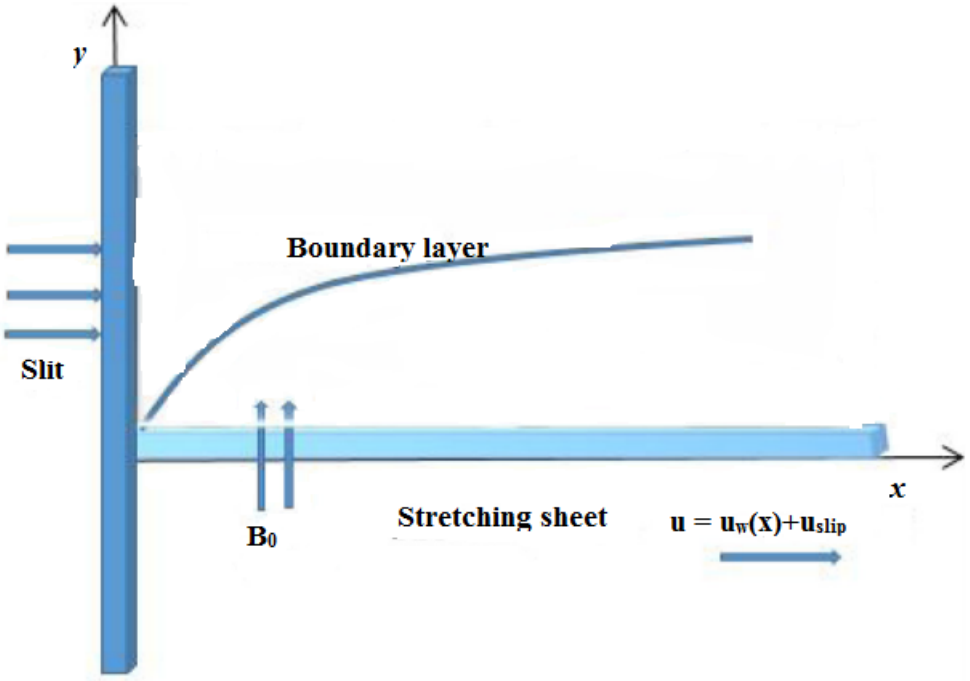

Figure 3.1: Geometry of the problem.

Assume that the fluid under discussion is taken as MHD two dimensional incompressible microploar's fluid which passes over porous stretching surface with slip velocity. The governing equations (3.1) - (3.4) are,

$$\frac{\partial u}{\partial x}+\frac{\partial v}{\partial y}=0, \tag{3.1}$$

$$u\frac{\partial u}{\partial x}+v\frac{\partial u}{\partial y}=\left(\frac{\mu+\kappa}{\rho}\right)\frac{\partial^2 u}{\partial y^2}-\frac{\kappa}{\rho}\frac{\partial N}{\partial y}+\frac{\sigma}{\rho}(E_0B_0-B_0^2u), \tag{3.2}$$

$$u\frac{\partial N}{\partial x}+v\frac{\partial N}{\partial y}=\frac{\gamma^*}{\rho j}\frac{\partial^2 N}{\partial y^2}-\frac{\kappa}{\rho j}(2N+\frac{\partial u}{\partial y}), \tag{3.3}$$

$$u\frac{\partial T}{\partial x}+v\frac{\partial T}{\partial y}=\frac{\kappa_1}{\rho C_p}\frac{\partial^2 T}{\partial y^2}+\frac{(uB_0-E_0)^2\,\sigma}{\rho C_p}+\frac{1}{\rho C_p}\frac{16\sigma^*}{3\kappa^*}T_\infty^*\frac{\partial^2 T}{\partial y^2}. \tag{3.4}$$

In (3.1) - (3.4), κ^* the mean absorption coefficient, σ^* the Stefen-Boltzman, T the temperature and B_0 the kinematic viscosity, B_0 the applied magnetic field strength, E_0 the applied electric field, $\nu=\frac{\mu}{\rho}$. The parameters κ and c_p are taken as constants and represents the permeability of porous media, the thermal conductivity and specific heat of the fluid respectively. The associated BCs for

the above system of equations are,

$$\left.\begin{aligned} &u = ax + \sigma^* \left[(\mu + \kappa) \frac{\partial u}{\partial y} + \kappa N \right], \quad v = v_w, \\ &N = -n\frac{\partial u}{\partial y}, \quad -\kappa \left(\frac{\partial T}{\partial y} \right) = h_f[T_f - T] \qquad \text{at} \quad y = 0, \\ &u \to 0, N \to 0, T \to T_\infty, \quad \text{as} y \to \infty. \end{aligned}\right\}$$

Here N, j, κ_1, α^*, v_w, and h_f represent the micro-rotation or angular velocity, micro inertia density, thermal conductivity, slip coefficient, suction/injection velocity, heat transfer coefficient respectively. Further, n is a constant and $0 \leq n \leq 1$. Now we convert the system of Eqs. (3.1) - (3.4) following the boundary conditions into a unitless form. For this purpose, we use the following similarity transformation.

$$\left.\begin{aligned} &\eta = \sqrt{\frac{a}{\nu}} y, \quad N = ax\sqrt{\frac{a}{\nu}} h(\eta), \quad u = \frac{\partial \psi}{\partial y}, \quad v = -\frac{\partial \psi}{\partial x} \\ &\psi(x, y) = \sqrt{a\nu} x f(\eta), \qquad \theta(\eta) = \frac{T - T_\infty}{T_f - T_\infty}. \end{aligned}\right\} \tag{3.5}$$

Here the parameters K, M, R, Ec, f_w, Pr and α are the material parameter, Hartmann number, radiation parameter, Eckert number, suction velocity, Prandtl number and slip parameter respectively. These quantities are formulated as follows:

$$K = \frac{\kappa}{\mu}, M^2 = \frac{\sigma B_0^2}{\rho a}, f_w = -(a\nu)^{\frac{-1}{2}} v_w, Pr = \frac{\mu C_p}{\kappa},$$
$$\alpha = \alpha^* \mu \sqrt{\frac{a}{\upsilon}}, E = \frac{E_0}{u_w B_0}, R = \frac{4\sigma^* T_\infty^3}{\kappa^* \kappa_1}.$$

The detailed procedure for the conversion of equations (3.1) - (3.4) has been described in the upcoming discussion.

$$
\begin{aligned}
\bullet \quad u &= \frac{\partial \psi}{\partial y} \\
&= \sqrt{av}xf'\left(\sqrt{\frac{a}{\nu}}y\right)\frac{\partial}{\partial y}\left(\sqrt{\frac{a}{\nu}}y\right) \\
&= \sqrt{av}xf'\left(\sqrt{\frac{a}{\nu}}y\right)\left(\sqrt{\frac{a}{\nu}}\right) = axf'(\eta). \\
\bullet \ \frac{\partial u}{\partial x} &= \frac{\partial}{\partial x}(axf'(\eta)) \\
&= af'(\eta). \qquad (3.6) \\
\bullet \quad v &= -\frac{\partial \psi}{\partial x} \\
&= -\frac{\partial}{\partial x}\left(\sqrt{a\nu}xf(\eta)\right) = -\sqrt{a\nu}f(\eta). \\
\bullet \ \frac{\partial v}{\partial y} &= -\frac{\partial}{\partial y}\left(\sqrt{a\nu}f\left(\sqrt{\frac{a}{\nu}}y\right)\right) \\
&= -\sqrt{a\nu}f'\left(\sqrt{\frac{a}{\nu}}y\right)\left(\sqrt{\frac{a}{\nu}}\right) \\
&= -af'(\eta). \qquad (3.7)
\end{aligned}
$$

Using (3.7) and (3.8) in (3.1),

$$\frac{\partial u}{\partial x} + \frac{\partial v}{\partial y} = af'(\eta) - af'(\eta) = 0.$$

Hence the equation of continuity is identically satisfied.

Now we include below, the procedure for the conversion of (3.2) into dimensionless form.

$$
\begin{aligned}
\bullet \quad \frac{\partial u}{\partial y} &= ax\frac{\partial}{\partial y}f'\left(\sqrt{\frac{a}{v}}y\right) = axf''\left(\sqrt{\frac{a}{\nu}}y\right)\frac{\partial}{\partial y}\left(\sqrt{\frac{a}{\nu}}y\right) = \frac{a^{\frac{3}{2}}x}{\sqrt{\nu}}f''(\eta). \\
\bullet \ u\frac{\partial u}{\partial x} &= (axf'(\eta))\,(af'(\eta)) = a^2x(f'(\eta))^2. \qquad (3.8) \\
\bullet \ v\frac{\partial u}{\partial y} &= -\sqrt{a\nu}f(\eta)\frac{a^{\frac{3}{2}}x}{\sqrt{\nu}}f''(\eta) = -a^2xf(\eta)f''(\eta). \qquad (3.9)
\end{aligned}
$$

Using (3.8) and (3.9), the left side of (3.2) becomes.

$$u\frac{\partial u}{\partial x}+v\frac{\partial u}{\partial y}=a^2x(f'(\eta))^2-a^2xf(\eta)f''(\eta)$$
$$=a^2x\left[(f'(\eta))^2-f(\eta)f''(\eta)\right].$$

To convert the right side of (3.2) into the dimensionless form, the following procedure has been followed.

- $$\frac{\partial u}{\partial y}=ax\frac{\partial}{\partial y}f'\left(\sqrt{\frac{a}{v}}y\right)=axf''\left(\sqrt{\frac{a}{\nu}}y\right)\frac{\partial}{\partial y}\left(\sqrt{\frac{a}{\nu}}y\right)$$
$$=\frac{a^{\frac{3}{2}}x}{\sqrt{\nu}}f''(\eta).$$
- $$\frac{\partial^2 u}{\partial y^2}=\frac{a^{\frac{3}{2}}x}{\sqrt{v}}f'''\left(\sqrt{\frac{a}{\nu}}y\right)\frac{\partial}{\partial y}\left(\sqrt{\frac{a}{\nu}}y\right)=\frac{a^2x}{\nu}f'''(\eta). \tag{3.10}$$
- $$\frac{\partial N}{\partial y}=ax\sqrt{\frac{a}{\nu}}\frac{\partial}{\partial y}h(\eta)=ax\sqrt{\frac{a}{\nu}}h'\eta\frac{\partial}{\partial y}\left(\sqrt{\frac{a}{\nu}}y\right)=\frac{a^2x}{\nu}h'(\eta).$$

(3.11)

- $$\left(\frac{\mu+\kappa}{\rho}\right)\frac{\partial^2 u}{\partial y^2}=\left(\frac{\mu+\kappa}{\rho}\right)\frac{a^2x}{\nu}f'''(\eta)=a^2x\left[\left(\frac{\mu+\kappa}{\rho\nu}\right)f'''(\eta)\right]$$
$$=a^2x\left[\left(\frac{\mu+\kappa}{\mu}\right)f'''(\eta)\right]=a^2x\left[\left(\frac{\mu}{\mu}+\frac{\kappa}{\mu}\right)f'''(\eta)\right].$$
$$=a^2\left(1+K\right)xf'''(\eta). \qquad \left(\because=\frac{\kappa}{\mu}\right) \tag{3.12}$$
- $$\frac{\kappa}{\rho}\frac{\partial N}{\partial y}=\frac{\kappa}{\rho}\frac{a^2x}{\nu}h'(\eta)=a^2x\left[\frac{\kappa}{\rho\nu}h'(\eta)\right]=a^2x\left[\frac{\kappa}{\mu}h'(\eta)\right]$$
$$=a^2Kxh'(\eta). \tag{3.13}$$
- $$\frac{\sigma}{\rho}(E_0B_0-B_0^2u)=\frac{\sigma}{\rho}\left(E_0B_0-B_0^2axf'(\eta)\right)$$
$$=a^2x\left[\frac{\sigma E_0B_0}{\rho a^2x}-\frac{\sigma B_0^2}{\rho a}f'(\eta)\right]$$
$$=a^2x\left[\left(\frac{\sigma B_0^2}{\rho a}\right)\left(\frac{E_0}{axB_0}\right)-\frac{\sigma B_0^2}{\rho a}f'(\eta)\right]$$
$$=a^2x\left[M^2E-M^2f'(\eta)\right] \quad \left(\because M^2=\frac{\sigma B_0^2}{\rho a},E=\frac{E_0}{axB_0}\right).$$

(3.14)

Using (3.10) - (3.14) in the right side of (3.2), we get

$$\left(\frac{\mu+\kappa}{\rho}\right)\frac{\partial^2 u}{\partial y^2}-\frac{\kappa}{\rho}\frac{\partial N}{\partial y}+\frac{\sigma}{\rho}(E_0B_0-B_0^2u)$$
$$=a^2x\left[(1+K)\,f'''(\eta)\right]+a^2x\left[Kh'(\eta)\right]+a^2x\left[M^2E-M^2f'(\eta)\right].$$

Hence the dimensionless form of (3.2) becomes.

$$ax^2\left[(f'(\eta))^2-f(\eta)f''(\eta)\right]=a^2x\left[(1+K)\,f'''(\eta)\right]+a^2x\left[Kh'(\eta)\right]$$
$$+a^2x\left[M^2E-M^2f'(\eta)\right]$$
$$\Rightarrow\left[(f'(\eta))^2-f(\eta)f''(\eta)\right]=\left[(1+K)\,f'''(\eta)\right]+\left[Kh'(\eta)\right]+\left[M^2E-M^2f'(\eta)\right]$$
$$\Rightarrow(1+K)f'''+ff''-f'^2-M^2f'+Kh'+M^2E=0.$$

Now we include below, the procedure for the conversion of (3.3) into dimensionless form as follows,

$$\bullet\quad\frac{\partial N}{\partial x}=a\sqrt{\frac{a}{\nu}}\frac{\partial}{\partial x}\left(xh\left(\sqrt{\frac{a}{\nu}}y\right)\right)=\frac{a^{\frac{3}{2}}}{\sqrt{\nu}}h(\eta).$$
$$\bullet\ u\frac{\partial N}{\partial x}=(axf'(\eta))\left(\frac{a^{\frac{3}{2}}}{\sqrt{\nu}}h(\eta)\right)=\frac{a^{\frac{5}{2}}}{\sqrt{v}}xf'(\eta)h(\eta).\tag{3.15}$$
$$\bullet\ v\frac{\partial N}{\partial y}=-\left(\sqrt{a\nu}f(\eta)\right)\frac{a^2x}{\nu}h'(\eta)$$
$$=-\frac{a^{\frac{5}{2}}}{\sqrt{\nu}}xf(\eta)h'(\eta).\tag{3.16}$$

Using (3.15) and (3.16), the left side of (3.3) gets the following form:

$$u\frac{\partial N}{\partial x}+v\frac{\partial N}{\partial y}=\frac{a^{\frac{5}{2}}}{\sqrt{\nu}}xf'(\eta)h(\eta)-\frac{a^{\frac{5}{2}}}{\sqrt{v}}xf(\eta)h'(\eta)$$
$$=\frac{a^{\frac{5}{2}}}{\sqrt{\nu}}x\left[f'(\eta)h(\eta)-f(\eta)h'(\eta)\right].\tag{3.17}$$

To convert the right side of (3.3) into dimensionless form, we proceed as follows.

- $$\frac{\partial^2 N}{\partial y^2} = \frac{\partial}{\partial y}\left(\frac{a^2 x}{\nu} h' \sqrt{\frac{a}{\nu}} y\right).$$
$$= \frac{a^2 x}{\nu} h''(\eta)\left(\sqrt{\frac{a}{\nu}}\right) = a^{\frac{5}{2}} \frac{x}{v^{\frac{3}{2}}} h''(\eta). \tag{3.18}$$
- $$\frac{\partial u}{\partial y} = a^{\frac{3}{2}} \frac{x}{\sqrt{\nu}} f''(\eta). \tag{3.19}$$
- $$\gamma^* = \left(\mu + \frac{\kappa}{2}\right) j = \mu\left(1 + \frac{\kappa}{2\mu}\right) j = \mu\left(1 + \frac{K}{2}\right) j. \tag{3.20}$$
- $$\frac{\gamma^*}{\rho j}\frac{\partial^2 N}{\partial y^2} = \frac{\mu\left(1+\frac{K}{2}\right) j}{\rho j} a^{\frac{5}{2}} \frac{x}{v^{\frac{3}{2}}} h''(\eta)$$
$$= a^{\frac{5}{2}} \frac{x}{\sqrt{\nu}}\left[\frac{\mu\left(1+\frac{K}{2}\right)}{\rho\nu} h''(\eta)\right]$$
$$= a^{\frac{5}{2}} \frac{x}{\sqrt{\nu}}\left[\frac{\mu\left(1+\frac{K}{2}\right)}{\mu} h''(\eta)\right]$$
$$= a^{\frac{5}{2}} \frac{x}{\sqrt{\nu}}\left[\left(1 + \frac{K}{2}\right) h''(\eta)\right]. \tag{3.21}$$

- $$\frac{\kappa}{\rho j}\left(2N + \frac{\partial u}{\partial y}\right) = \frac{\kappa}{\rho j}\left[2ax\sqrt{\frac{a}{\nu}} h(\eta) + a^{\frac{3}{2}} \frac{x}{\sqrt{v}} f''(\eta)\right]$$
$$= a^{\frac{5}{2}} \frac{x}{\sqrt{\nu}}\left[\frac{\kappa}{\rho j a}\left(2h(\eta) + f''(\eta)\right)\right]$$
$$= a^{\frac{5}{2}} \frac{x}{\sqrt{\nu}}\left[\frac{\kappa}{\rho a \frac{\nu}{a}}\left(2h(\eta) + f''(\eta)\right)\right] \qquad \left(\because j = \frac{\nu}{a}\right)$$
$$= a^{\frac{5}{2}} \frac{x}{\sqrt{\nu}}\left[\frac{\kappa}{\rho\nu}\left(2h(\eta) + f''(\eta)\right)\right]$$
$$= a^{\frac{5}{2}} \frac{x}{\sqrt{\nu}}\left[K\left(2h(\eta) + f''(\eta)\right)\right]. \tag{3.22}$$

Using (3.18) and (3.22) the dimensionless form of right side (3.3) is as follows.

$$\frac{\gamma^*}{\rho j}\frac{\partial^2 N}{\partial y^2} - \frac{\kappa}{\rho j}\left(2N + \frac{\partial u}{\partial y}\right)$$
$$= a^{\frac{5}{2}} \frac{x}{\sqrt{\nu}}\left[\left(1 + \frac{K}{2}\right) h''(\eta)\right] - a^{\frac{5}{2}} \frac{x}{\sqrt{\nu}}\left[K\left(2h(\eta) + f''(\eta)\right)\right]$$

Therefore the dimensionless form (3.3) becomes:

$$\Rightarrow \frac{a^{\frac{5}{2}}}{\sqrt{\nu}} x \left[f'(\eta)h(\eta) - f(\eta)h'(\eta)\right] = a^{\frac{5}{2}} \frac{x}{\sqrt{\nu}} \left(1 + \frac{K}{2}\right) h''(\eta)$$
$$- a^{\frac{5}{2}} \frac{x}{\sqrt{\nu}} \left[K\left(2h(\eta) + f''(\eta)\right)\right]$$
$$\Rightarrow \left[f'(\eta)h(\eta) - f(\eta)h'(\eta)\right] = \left(1 + \frac{K}{2}\right) h''(\eta) - K\left(2h(\eta) + f''(\eta)\right)$$
$$\Rightarrow \left(1 + \frac{K}{2}\right) h'' + fh' - f'h - K\left(2h + f''\right) = 0$$

Now we include below, the procedure for the conversion of (3.4) into the dimensionless form.

$$\bullet \quad \theta(\eta) = \frac{T - T_\infty}{T_f - T_\infty}$$

$$\Rightarrow \quad T = (T_f - T_\infty)\theta(\eta) + T_\infty. \tag{3.23}$$

$$\bullet \quad \frac{\partial T}{\partial x} = 0. \tag{3.24}$$

$$\bullet \quad u\frac{\partial T}{\partial x} = 0. \tag{3.25}$$

$$\bullet \quad \frac{\partial T}{\partial y} = \sqrt{\frac{a}{\nu}} \left(T_f - T_\infty\right)\theta'(\eta). \tag{3.26}$$

$$\bullet \quad v\frac{\partial T}{\partial y} = -a\left(T_f - T_\infty\right)\theta'(\eta)f(\eta). \tag{3.27}$$

Using (3.23) and (3.27) the left side of (3.28) gets the following form:

$$u\frac{\partial T}{\partial x} + v\frac{\partial T}{\partial y} = 0 - \theta'(\eta)f(\eta)a(T_f - T_\infty)$$
$$= -a(T_f - T_\infty)\theta'(\eta)f(\eta). \tag{3.28}$$

To convert the right side of (3.4) into the dimensionless form, we proceed as follows.

$$
\begin{aligned}
\bullet \qquad \frac{\partial^2 T}{\partial y^2} &= \frac{a}{\nu}\,(T_f - T_\infty)\theta''(\eta).\\
\bullet \qquad \frac{\kappa_1}{\rho C_p}\frac{\partial^2 T}{\partial y^2} &= \frac{\kappa_1}{\rho c_p}\frac{a}{\nu}\,(T_f - T_\infty)\theta''(\eta). \qquad (3.29)\\
\bullet \qquad \frac{(uB_0 - E_0)^2\,\sigma}{\rho c_p} &= \frac{(u^2B_0^2 + E_0^2 - 2E_0uB_0)}{\rho C_p}\sigma\\
&= \frac{(a^2x^2(f'(\eta))^2B_0^2 + E_0^2 - 2E_0axf'(\eta)B_o)}{\rho c_p}\sigma \quad (\because u = axf'(\eta))\\
&= (ax)^2B_0^2\frac{\left((f'(\eta))^2 + \frac{E_0^2}{(ax)^2B_0^2} - \frac{2E_0}{(ax)B_0}f'(\eta)\right)}{\rho C_p}\sigma \quad (\because u_w = ax)\\
&= u_w^2B_0^2\sigma\frac{((f'(\eta))^2 + E^2 - 2Ef'(\eta))}{\rho C_p}. \qquad \left(\because E = \frac{E_0}{(ax)B_0}\right).
\end{aligned}
\qquad (3.30)
$$

$$
\begin{aligned}
\bullet\ \frac{1}{\rho c_p}\frac{16\sigma^*}{3\kappa^*}T_\infty^*\frac{\partial^2 T}{\partial y^2} &= \frac{1}{\rho C_p}\frac{16\sigma^*}{3\kappa^*}T_\infty^*\frac{a}{\nu}(\eta)\,(T_f - T_\infty)\,\theta''\\
&= \frac{4\kappa_1}{3\rho C_p}\frac{4\sigma^*T_\infty^*}{\kappa_1\kappa^*}\frac{a}{\nu}\,(T_f - T_\infty)\,\theta''(\eta)\\
&= \frac{4}{3}\frac{a}{\nu}\frac{\kappa_1 R}{\rho C_p}\theta''(\eta)\,(T_f - T_\infty)\,. \qquad \left(\because R = \frac{4\sigma^*}{\kappa_1\kappa^*}T_\infty^*\right) \qquad (3.31)
\end{aligned}
$$

Using (3.29)-(3.31), the dimensionless form of the right side of (3.4) is as follows.

$$
\begin{aligned}
&\frac{\kappa_1}{\rho C_p}\frac{\partial^2 T}{\partial y^2} + \frac{(uB_0 - E_0)^2\,\sigma}{\rho c_p} + \frac{1}{\rho C_p}\frac{16\sigma^*}{3\kappa^*}T_\infty^*\frac{\partial^2 T}{\partial y^2}\\
&= \frac{\kappa_1}{\rho C_p}\frac{a}{\nu}\,(T_f - T_\infty)\,\theta''(\eta) + u_w^2B_0^2\sigma\frac{((f'(\eta))^2 + E^2 - 2Ef'(\eta))}{\rho C_p}\\
&\quad + \frac{4}{3}\frac{a}{\nu}\frac{\kappa_1 R}{\rho C_p}\theta''(\eta)\,(T_f - T_\infty)\\
&= a\,(T_f - T_\infty)\left[\frac{\kappa_1}{\rho\nu C_p}\left(1 + \frac{4R}{3}\right)\theta''(\eta)\right]\\
&\quad + a\,(T_f - T_\infty)\left[\left(\frac{u_w^2}{C_p\,(T_f - T_\infty)}\right)\left(\frac{B_0^2\sigma}{\rho a}\right)\left(f'^2(\eta) + E^2 - 2Ef'(\eta)\right)\right]\\
&= a\,(T_f - T_\infty)\left[\frac{\kappa_1}{\mu C_p}\left(1 + \frac{4R}{3}\right)\theta''(\eta) + EcM^2\left(f'^2(\eta) + E^2 - 2Ef'(\eta)\right)\right]\\
&\qquad \left(\because Ec = \frac{u_w^2}{C_p\,(T_f - T_\infty)}, M^2 = \frac{B_0^2\sigma}{\rho a}\right)
\end{aligned}
$$

$$= \frac{a\kappa_1}{\mu C_p}(T_f - T_\infty)\left[\left(1+\frac{4R}{3}\right)\theta''(\eta) + \frac{\mu C_p}{\kappa_1} EcM^2\left(f'^2(\eta) + E^2 - 2Ef'(\eta)\right)\right]$$
$$= \frac{a\kappa_1}{\mu C_p}(T_f - T_\infty)\left[\left(1+\frac{4R}{3}\right)\theta''(\eta) + PrEcM^2\left(f'^2(\eta) + E^2 - 2Ef'(\eta)\right)\right].$$
$$\left(\because Pr = \frac{\mu C_p}{\kappa_1}\right) \tag{3.32}$$

Therefore the dimensionless form of (3.4) becomes:

$$u\frac{\partial T}{\partial x} + v\frac{\partial T}{\partial y} = \frac{\kappa_1}{\rho C_p}\frac{\partial^2 T}{\partial y^2} + \frac{(uB_0 - E_0)^2\sigma}{\rho C_p} + \frac{1}{\rho C_p}\frac{16\sigma^*}{3\kappa^*}T_\infty^*\frac{\partial^2 T}{\partial y^2}$$
$$- a(T_f - T_\infty)\theta'(\eta)f(\eta) = \frac{a\kappa_1}{\mu C_p}(T_f - T_\infty)\left[\left(1+\frac{4R}{3}\right)\theta''(\eta)\right]$$
$$+ \frac{a\kappa_1}{\mu C_p}(T_f - T_\infty)\left[PrEcM^2\left(f'^2(\eta) + E^2 - 2Ef'(\eta)\right)\right]$$
$$\Rightarrow -\frac{\mu C_p}{\kappa_1}\theta'(\eta)f(\eta) = \left(1+\frac{4R}{3}\right)\theta''(\eta) + PrEcM^2\left(f'^2(\eta) + E^2 - 2Ef'(\eta)\right)$$
$$\Rightarrow -Pr\theta'(\eta)f(\eta) = \left(1+\frac{4R}{3}\right)\theta''(\eta) + PrEcM^2\left(f'^2(\eta) + E^2 - 2Ef'(\eta)\right)$$
$$\Rightarrow \left(1+\frac{4R}{3}\right)\theta'' + Pr\theta' f + PrEcM^2\left(f'^2 + E^2 - 2Ef'\right) = 0$$

Rewriting the converted ODEs together,

$$(1+K)f''' + ff'' - f'^2 + Kh' - M^2 f' + M^2 E = 0, \tag{3.33}$$
$$\left(1+\frac{K}{2}\right)h'' + fh' - f'h' - K(2h + f'') = 0, \tag{3.34}$$
$$\left(1+\frac{4R}{3}\right)\theta'' + Prf\theta' + M^2 Ec[f'^2 + E^2 - 2Ef'] = 0, \tag{3.35}$$

The BCs are of the form,

$$
\begin{aligned}
\bullet \quad v &= \nu_w, \\
\Rightarrow -\sqrt{a}\nu f(\eta) &= \nu_w \\
\Rightarrow f(\eta) &= -\frac{\nu_w}{\sqrt{a}\nu} \\
\Rightarrow f(\eta) &= -(a\nu)^{-\frac{1}{2}}\nu_w \\
\Rightarrow f(\eta) &= f_w. \qquad \left(\because f_w = -(a\nu)^{-\frac{1}{2}}\nu_w\right) \\
\bullet \quad N &= -n\frac{\partial u}{\partial y} \\
\Rightarrow ax\sqrt{\frac{a}{\nu}}h(\eta) &= -n\frac{a^{\frac{3}{2}}}{\sqrt{\nu}}xf''(\eta) \\
\Rightarrow h(\eta) &= -nf''(\eta). \\
\bullet \quad u &= ax + \alpha^*\left[(\mu+\kappa)\frac{\partial u}{\partial y} + \kappa N\right] \\
\Rightarrow axf'(\eta) &= ax + \alpha^*\left[(\mu+\kappa)\frac{a^{\frac{3}{2}}}{\sqrt{\nu}}xf''(\eta) + \kappa ax\sqrt{\frac{a}{\nu}}h(\eta)\right] \\
\Rightarrow f'(\eta) &= 1 + \alpha^*\left[(\mu+\kappa)\sqrt{\frac{a}{\nu}}f''(\eta) + \kappa\sqrt{\frac{a}{\nu}}h(\eta)\right] \\
\Rightarrow f'(\eta) &= 1 + \alpha^*\mu\sqrt{\frac{a}{\nu}}f''(\eta) + \alpha^*\kappa\sqrt{\frac{a}{\nu}}f''(\eta) + \alpha^*\kappa\sqrt{\frac{a}{\nu}}h(\eta) \\
\Rightarrow f'(\eta) &= 1 + \alpha f''(\eta) + \alpha K f''(\eta) + \alpha K h(\eta) \qquad \left(\because K = \frac{\kappa}{\mu}, \alpha = \alpha^*\mu\sqrt{\frac{a}{\nu}}\right) \\
\Rightarrow f'(\eta) &= 1 + \alpha(1+K)f''(\eta) - \alpha K n f''(\eta) \quad (\because h(\eta) = -nf''(\eta)) \\
\Rightarrow f'(\eta) &= 1 + \alpha(1+K-Kn)f''(\eta) \\
\Rightarrow f'(\eta) &= 1 + \alpha\left(1 + K(1-n)\right)f''(\eta). \\
\bullet \quad h_t\left[T_f - T\right] &= -\kappa\frac{\partial T}{\partial y} \\
\Rightarrow h_t\left[T_f - T\right] &= -\kappa\left[\theta'(\eta)\sqrt{\frac{a}{\nu}}(T_f - T_\infty)\right] \\
\Rightarrow \theta'(\eta) &= -\frac{h_t\left(T_f - T\right)}{\sqrt{\frac{a}{\nu}}(T_f - T_\infty)} \\
\Rightarrow \theta'(\eta) &= -\frac{h_f}{\kappa}\sqrt{\frac{a}{\nu}}\left[T_f - \theta(\eta)\left(T_f - T_\infty\right) - T_\infty\right] \\
\Rightarrow \theta'(\eta) &= -\gamma\left(1 - \theta(\eta)\right). \qquad \left(\because \gamma = \frac{h}{\kappa\sqrt{\frac{a}{\nu}}}\right)
\end{aligned}
$$

$$
\begin{aligned}
\bullet \qquad u &= axf'(\eta), \qquad u \to 0,\ as\ y \to \infty \\
\Rightarrow\ axf'(\infty) &= 0 \\
\Rightarrow\ f'(\infty) &= 0. \\
\bullet \qquad N &= ax\sqrt{\frac{a}{\nu}}h(\eta), \qquad N \to 0,\ as\ y \to \infty \\
\Rightarrow ax\sqrt{\frac{a}{\nu}}h(\eta) &= 0 \\
\Rightarrow\ h(\infty) &= 0. \\
\bullet \qquad \theta(\eta) &= \frac{T - T_\infty}{T_f - T_\infty}, \qquad T \to T_\infty\ as\ y \to \infty \\
\Rightarrow\ \theta(\infty) &= 0.
\end{aligned}
$$

Rewriting the converted ODEs together,

$$
\left.
\begin{aligned}
&f(\eta) = f_w,\ f'(\eta) = 1 + \alpha(1+K)f''(\eta), \\
&h(\eta) = -nf''(\eta),\ \theta'(\eta) = -\gamma(1-\theta(\eta)),\ \text{at } \eta = 0, \\
&f'(\eta) = 0, \quad h(\eta) = 0, \quad \theta(\eta) = 0, \quad \text{as} \quad \eta \to \infty.
\end{aligned}
\right\} \tag{3.36}
$$

The local skin friction and the Nuselt numbers are characterized as

$$C_{fx} = \frac{2\tau_w}{\rho(ax)^2}, \tag{3.37}$$

$$Nu_x = \frac{xq_w}{\kappa(T_f - T_\infty)}. \tag{3.38}$$

where τ_w and q_w are given by

$$\tau_w = \left((\mu + \kappa)\frac{\partial u}{\partial y} + \kappa N\right)_{y=0}, \tag{3.39}$$

$$q_w = -\kappa_1 \left(\frac{\partial T}{\partial y}\right)_{y=0}. \tag{3.40}$$

The dimensionless form of the above quantities becomes

$$\frac{1}{2}C_{fx}Re_x^{\frac{1}{2}} = (1 + (1-n)K)f''(0), \tag{3.41}$$

$$NuRe_x{}^{-1/2}x = -\frac{1}{3}[3 + 4R_d\left((Q_w - 1)\,\theta(0) + 1\right)^3]\theta'(0). \tag{3.42}$$

Where the local Reynolds number is defined as

$$Re_x = ux/v. \tag{3.43}$$

3.3 Solution methodology

The analytic solution of the boundary value problem (3.33) - (3.36) cannot be found because these equation are non-linear and coupled. So, we use a numerical technique, i.e.,the shooting scheme with fourth order Runge Kutta method. In order to solve the system of ODEs (3.33) - (3.35), with boundary conditions (3.36), utilizing the shooting method, first of all we have to change these equations into a system of first order differential expressions. Let us use the following notations.

$$\left.\begin{aligned} f = y_1, \quad f' = y_2, \quad f'' = y_3, \\ h = y_4, \quad h' = y_5, \\ \theta = y_6, \quad \theta' = y_7. \end{aligned}\right\} \tag{3.44}$$

The system of equation (3.33) - (3.35) following the boundary limits are (3.36) changed into a system of seven first order differential expressions.

$$\left.\begin{aligned} y_1' &= y_2, & y_1(0) &= f_w, \\ y_2' &= y_3, & y_2(0) &= 1 + \alpha(1+K)s, \\ y_3' &= \frac{(y_2^2 - y_1 y_3 - K y_5 + M^2 y_2 - M^2 E)}{(1+K)}, & y_3(0) &= s, \\ y_4' &= y_5, & y_4(0) &= -ns, \\ y_5' &= \frac{2\left(y_2 y_5 + K\left(2y_4 + y_3\right) - y_1 y_5\right)}{(2+K)}, & y_5(0) &= t, \\ y_6' &= y_7, & y_6(0) &= u, \\ y_7' &= \frac{3\left(-Pr y_1 y_7 - M^2 Ec\left[y_2^2 + E^2 - 2E y_2\right]\right)}{(3+4R)}, & y_7(0) &= -\gamma(1-u). \end{aligned}\right\} \tag{3.45}$$

In the above system of equations (3.45), the missing initial conditions s, t, and u are to be chosen such that

$$\left.\begin{aligned} y_2(\eta_\infty, s, t, u) &= 0, \\ y_4(\eta_\infty, s, t, u) &= 0, \\ y_6(\eta_\infty, s, t, u) &= 0. \end{aligned}\right\} \tag{3.46}$$

To solve the system of equations (3.46), we use the Newton's method which has the following iterative scheme

$$\begin{pmatrix} s^{(n+1)} \\ t^{(n+1)} \\ u^{(n+1)} \end{pmatrix} = \begin{pmatrix} s^{(n)} \\ t^{(n)} \\ u^{(n)} \end{pmatrix} - \begin{pmatrix} \frac{\partial y_2}{\partial s} & \frac{\partial y_2}{\partial t} & \frac{\partial y_2}{\partial u} \\ \frac{\partial y_4}{\partial s} & \frac{\partial y_4}{\partial t} & \frac{\partial y_4}{\partial u} \\ \frac{\partial y_6}{\partial s} & \frac{\partial y_6}{\partial t} & \frac{\partial y_6}{\partial u} \end{pmatrix}^{-1}_{(\eta_\infty, s^{(n)}, t^{(n)}, u^{(n)})} \begin{pmatrix} y_2^{(n)} \\ y_4^{(n)} \\ y_6^{(n)} \end{pmatrix}_{(\eta_\infty, s^{(n)}, t^{(n)}, u^{(n)})}$$

Let us now use the following notations:

$$\begin{aligned} \frac{\partial y_1}{\partial s} &= y_8, \frac{\partial y_2}{\partial s} = y_9, \ldots \quad \frac{\partial y_7}{\partial s} = y_{14}, \\ \frac{\partial y_1}{\partial t} &= y_{15}, \frac{\partial y_2}{\partial t} = y_{16}, \ldots \quad \frac{\partial y_7}{\partial t} = y_{21}, \\ \frac{\partial y_1}{\partial u} &= y_{22}, \frac{\partial y_2}{\partial u} = y_{23}, \ldots \quad \frac{\partial y_7}{\partial u} = y_{28}, \end{aligned}$$

With these new notation, the Newton's iterative scheme get the following form.

$$\begin{pmatrix} s^{(n+1)} \\ t^{(n+1)} \\ u^{(n+1)} \end{pmatrix} = \begin{pmatrix} s^{(n)} \\ t^{(n)} \\ u^{(n)} \end{pmatrix} - \begin{pmatrix} y_9 & y_{16} & y_{23} \\ y_{11} & y_{18} & y_{25} \\ y_{13} & y_{20} & y_{27} \end{pmatrix}^{-1}_{(\eta_\infty, s^{(n)}, t^{(n)}, u^{(n)})} \begin{pmatrix} y_2^{(n)} \\ y_4^{(n)} \\ y_6^{(n)} \end{pmatrix}_{(\eta_\infty, s^{(n)}, t^{(n)}, u^{(n)})}$$

For the execution of the above iterative scheme, we differentiate equations (3.45) w.r.t each variable s, t, and u to have another IVP consisting of system of twenty one ODEs. Rewriting all the twenty eight ODEs together along with the corresponding ICs we have the following IVP.

$$y_1' = y_2, \qquad y_1(0) = f_w,$$

$$y_2' = y_3, \qquad y_2(0) = 1 + \alpha(1+K)s,$$

$$y_3' = \frac{1}{(1+K)}\left(y_2^2 - y_1 y_3 - K y_5 + M^2 y_2 - M^2 E\right), \qquad y_3(0) = s,$$

$$y_4' = y_5, \qquad y_4(0) = -ns,$$

$$y_5' = \frac{2}{(2+K)}\left(y_2 y_5 + K\left(2y_4 + y_3\right) - y_1 y_5\right), \qquad y_5(0) = t,$$

$$y_6' = y_7, \qquad y_6(0) = u,$$

$$y_7' = \frac{3}{(3+4R)}\left(-Pr y_1 y_7 - M^2 Ec\left[y_2^2 + E^2 - 2E y_2\right]\right), \qquad y_7(0) = -\gamma(1-u),$$

$$y_8' = y_9, \qquad y_8(0) = 0,$$

$$y_9' = y_{10}, \qquad y_9(0) = \alpha(1+K),$$

$$y_{10}' = \frac{1}{(1+K)}\left(2y_2 y_9 + M^2 y_9 - y_9 y_{10} - y_3 y_8 - K y_{12}\right), \qquad y_{10}(0) = 1,$$

$$y_{11}' = y_{12}, \qquad y_{11}(0) = -n,$$

$$y_{12}' = \frac{2}{(2+K)}\left(y_2 y_{11} + y_4 y_9 + K\left(2y_{11} + y_{10}\right) - y_1 y_{12} - y_5 y_8\right), \qquad y_{12}(0) = 0,$$

$$y_{13}' = y_{14}, \qquad y_{13}(0) = 0,$$

$$y_{14}' = \frac{3}{(3+4R)}\left(-Pr(y_1 y_{14} + y_7 y_8) - M^2 Ec\left[2y_2 y_9 - 2E y_9\right]\right), \qquad y_{14}(0) = 0,$$

$$y_{15}' = y_{16}, \qquad y_{15}(0) = 0,$$

$$y_{16}' = y_{17}, \qquad y_{16}(0) = 0,$$

$$y_{17}' = \frac{1}{(1+K)}\left(2y_2 y_{16} + M^2 y_{16} - y_1 y_{17} - y_{15} y_3 - K y_{19}\right), \qquad y_{17}(0) = 0,$$

$$y_{18}' = y_{19}, \qquad y_{18}(0) = 0,$$

$$y_{19}' = \frac{2}{(2+K)}\left(y_2 y_{18} + y_4 y_{16} + K\left(2y_{18} + y_{17}\right) - y_1 y_{19} - y_5 y_{15}\right), \qquad y_{19}(0) = 1,$$

$$y_{20}' = y_{21}, \qquad y_{20}(0) = 0,$$

$$
\begin{aligned}
&y_{21}' = \\
&\frac{3}{(3+4R)}\left(-Pr(y_1y_{21}+y_7y_{15}) - M^2Ec\left[2y_2y_{16}-2Ey_{16}\right]\right), && y_{21}(0)=0\\
&y_{22}' = y_{23}, && y_{22}(0)=0,\\
&y_{23}' = y_{24}, && y_{24}(0)=0,\\
&y_{24}' = \\
&\frac{1}{(1+K)}\left(2y_2y_{23}+M^2y_{23}-y_1y_{24}-y_{22}y_3-Ky_{26}\right), && y_{24}(0)=0,\\
&y_{25}' = y_{26}, && y_{26}(0)=0,\\
&y_{26}' = \\
&\frac{2}{(2+K)}\left(y_2y_{25}+y_4y_{23}+K\left(2y_{25}+y_{24}\right)-y_1y_{26}-y_5y_{22}\right), && y_{26}(0)=0,\\
&y_{27}' = y_{28}, && y_{27}(0)=1,\\
&y_{28}' = \\
&\frac{3}{(3+4R)}\left(-Pr(y_1y_{28}+y_7y_{22}) - M^2Ec\left[2y_2y_{23}-2Ey_{23}\right]\right), && y_{28}(0)=0.
\end{aligned}
$$

The shooting method requires the initial guess for $y_3(0)$, $y_5(0)$ and $y_6(0)$, and by the Newton's mechanism we update each guess until we obtain an approximate result for our problem. To strengthen the reliability of the obtained numerical results by the shooting method , we compare these by the numerical results acquired by the MATLAB solver bvp4c. and found them in excellent agreement.

3.4 Results and discussion

The objective of this section is to analyze the numerical results displayed in the shape of graphs and tables. The computations are carried out for various values of the material parameter K, Hartmann number M, electric parameter E, radiation parameter R, Eckert number Ec, suction velocity f_w, slip parameter α, and Prandtl number Pr and the impact of these parameters on the velocity, microrotation and temperature profiles is also discussed in detail.

3.4.1 Impact of slip parameter and suction parameter on the unitless velocity profile

The effect of slip parameter α on the dimensionless velocity profile $f'(\eta)$ is presented in Figure 3.2. Increasing the values of the slip parameter α reduces the velocity field and particular boundary thickness as depicted in Figure 3.2.. The impact of the section parameter f_w on the dimensionless velocity profile $f'(\eta)$ is presented in Figure 3.3. Velocity profile diminishes and accompanied with boundary layer width increases for gradually growing values of the suction parameter f_w.

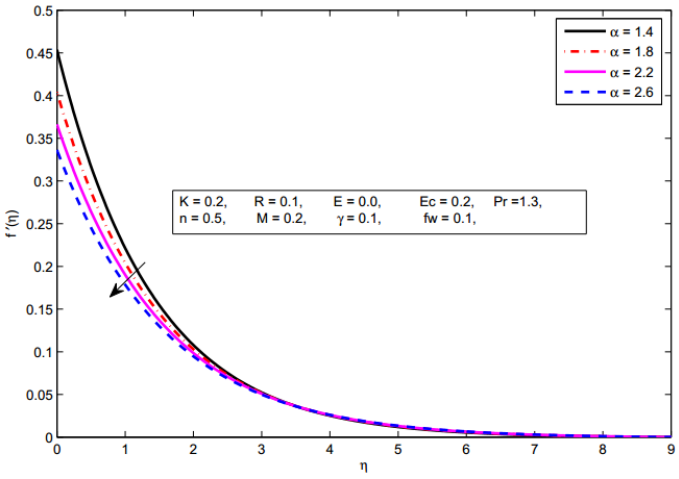

Figure 3.2: Impact of α on the unitless velocity $f'(\eta)$

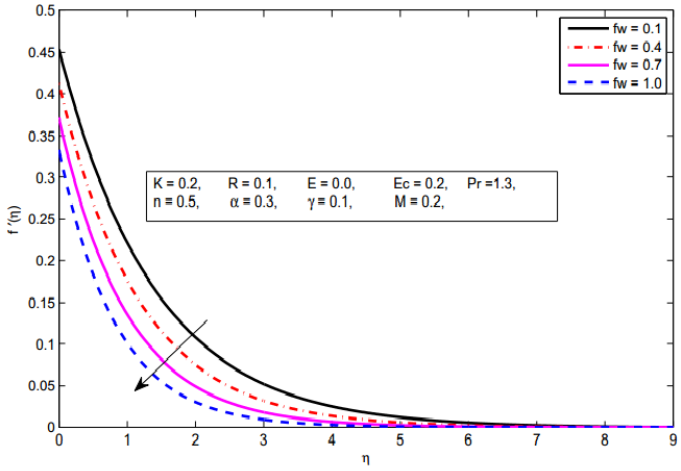

Figure 3.3: Impact of f_w on the unitless velocity $f'(\eta)$.

3.4.2 Impact of material parameter on the unitless velocity profile and dimensionless microrotation profile

The impact of the material parameter K on the dimensionless velocity profile $f'(\eta)$ is presented in Figure 3.4. By increasing K, the velocity field reduces in the lower half of the surface whereas it enhances in the upper half. The velocity is going to reduce initially with the mounting values of the material parameter K. However for $\eta > 1$ there is an elevation in the velocity profile. Figure 3.5 shows the impact of the material parameter K on the dimensionless micrototation profile $h(\eta)$. By increasing the values of K the microrotation decreases.

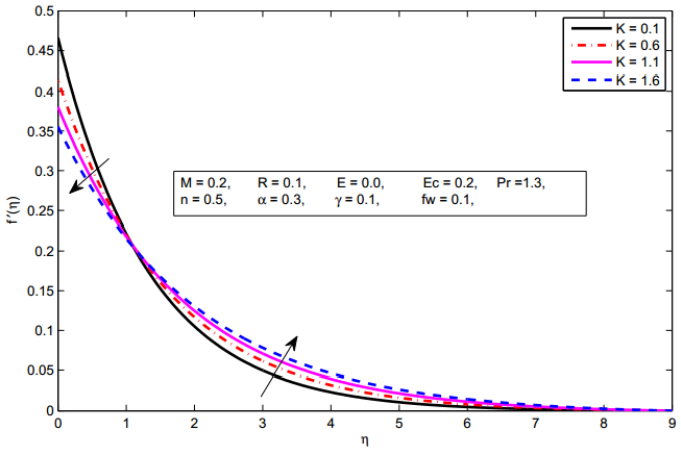

Figure 3.4: Impact of K on the unitless velocity $f'(\eta)$.

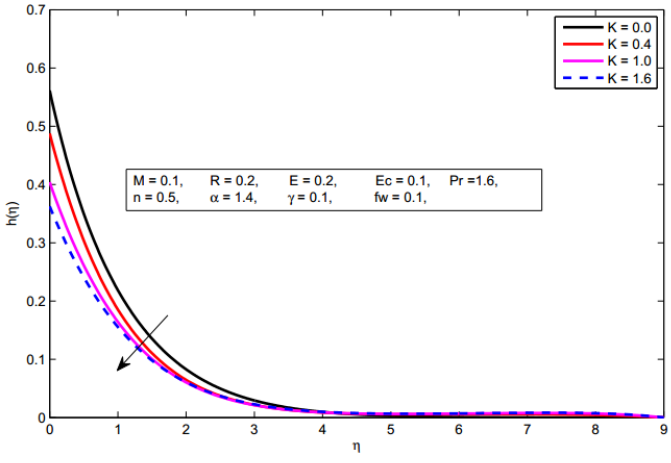

Figure 3.5: Impact of K on the unitless microrotation $h(\eta)$.

3.4.3 Impact of Hartmann number on the unitless velocity profile and dimensionless energy profile

Figure 3.6 and 3.7 depict the impact of Hartman number M on the velocity profile $f'(\eta)$ and the dimensionless energy profile $\theta(\eta)$. It is shows that the huge values of the magnetic parameter M case a fall down the velocity profile $f'(\eta)$ and an increase in the dimensionless energy profile $\theta(\eta)$, since the magnetic field introduces a force i.e. the Lorentz force which opposes the stream and the velocity distribution.

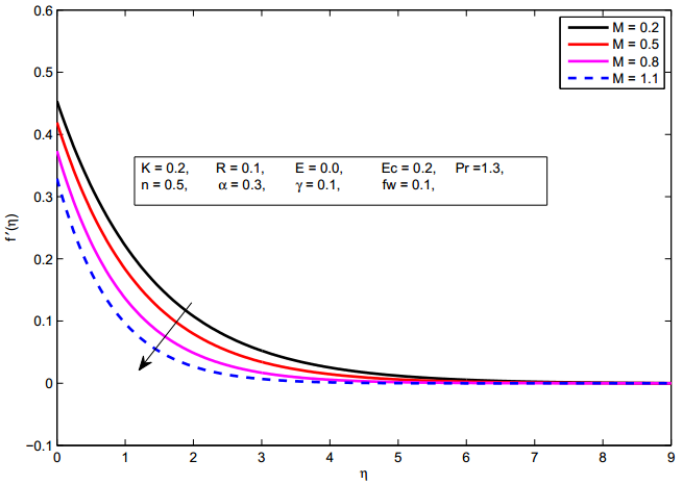

Figure 3.6: Impact of M on the unitless velocity $f'(\eta)$.

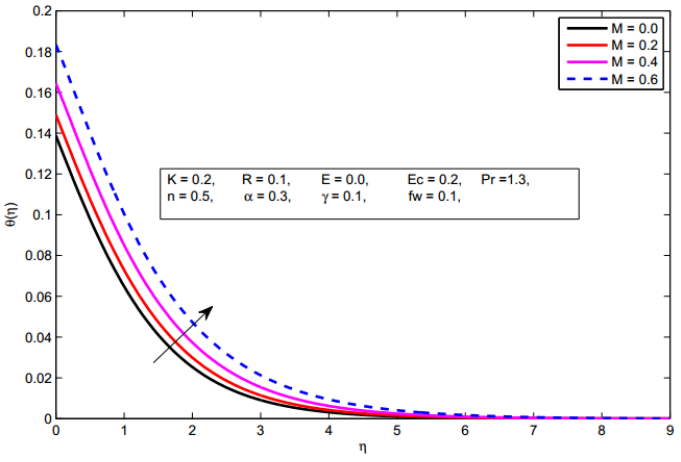

Figure 3.7: Impact of M on the unitless energy $\theta(\eta)$.

3.4.4 Impact of Biot number and Eckert number on the dimensionless energy profile

Figure 3.8 demonstrates the impact of the Biot number γ on the temperature $\theta(\eta)$. We notice that the enhanced values of Biot number γ cause a higher energy and thicker the thermal boundary layer thickness. Figure 3.9 displays the influence of Eckert number E_c on the energy profile. Energy profile increases when the Eckert number is increased. Due to friction, the heat energy is kept in owing to accelerating values of Eckert number, which results in the enhancement of the temperature profile.

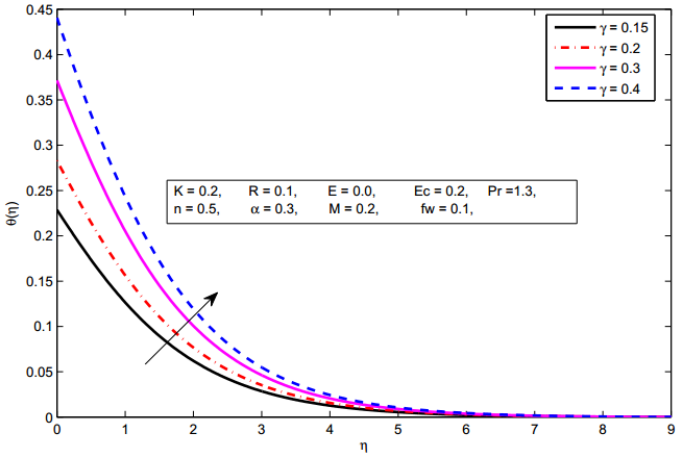

Figure 3.8: Impact of γ on the unitless energy θ.

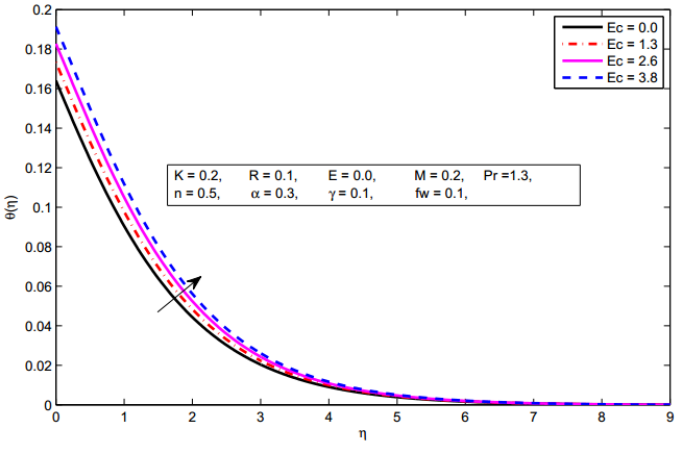

Figure 3.9: Impact of Ec on the unitless energy $\theta(\eta)$.

3.4.5 Skin-friction coefficient and Nusselt number

The Nusselt number Nu_x is of great interest for engineers. In Table 3.1, the numerical analysis of Nu_x for different physical parameters under discussion, is displayed. Here, we use the shooting technique with the Runge-Kutta fourth order mechanism. We compare the results obtained by the shooting method with those obtained by the matlab code bvp4c and both are found in an excellent agreement. It is found that the inflation in the radiation parameter R, γ, electric parameter E, Eckert number Ec, and Prandtl number Pr results a rise in the Nusselt number. Moreover, the Nusselt number has inverse relation with Hartman number M and the slip parameter α.

							$NuRe_x^{-1/2}$		
Parameters							Ramzan et al. [36]	Present	
M	R	E	α	γ	Ec	Pr	HAM	Shooting	bvp4c
0.2	0.1	0.2	0.1	0.1	0.2	1.0	0.08591	0.0851094	0.0851409
0.3							0.08595	0.0848762	0.0848762
0.6							0.08490	0.0837395	0.0837395
0.9							0.08381	0.0833257	0.0820566
0.2	0.3						0.08540	0.0833257	0.0833257
	0.6						0.84400	0.0811546	0.0811546
	0.9						0.08351	0.0794392	0.0794392
	0.1	0.3					0.08580	0.0851475	0.0851475
		0.6					0.08605	0.0849750	0.0849750
		0.9					0.08599	0.0833698	0.0843369
		0.2	0.3				0.08515	0.0842594	0.0842594
			0.6				0.08440	0.0833190	0.0833190
			0.9				0.08339	0.0825988	0.0825988
			0.1	0.3			0.20212	0.1972475	0.1972475
				0.6			0.34401	0.2941681	0.2941681
				0.9			0.36662	0.3517867	0.3517867
				0.1	0.3		0.08544	0.0850035	0.0850035
					0.6		0.08455	0.0847210	0.0847210
					0.9		0.08355	0.0844384	0.0844384
					0.2		0.08745	0.0872886	0.0872828
						2.0	0.08951	0.0901095	0.0901959
						3.0	0.09194	0.0922698	0.0922698
						4.0	0.09340	0.0935145	0.0935145

Table 3.1: Numerical results of $NuRe_x^{-1/2}$ for different values of Pr, K, M, R, E, α, γ, and Ec

3.5 Summary

In this chapter, the numerical study of the flow of micropoler fluid past a porous stretching sheet in the presence of Joule heating, partial slip and magnatohydrodynamic (MHD), is presented. The properties of the fluid like viscosity and thermal conductivity are taken independent of temperature. The dimensionless velocity, dimensionless temperature and dimensionless micro-rotation are analyzed and presented in the form of graphs and tables. We present the Nusselt number in the tabular form for different values of the distinctive physical parameters. From the above study, we can make the following conclusions.

- The material parameter K diminishes the micro-rotation and distributions of velocity.
- The slip parameter α diminishes the micro-rotation and the velocity distributions.
- The energy failed with its boundary layer thickness inflated against the mounting values of the electrical field parameter E.
- The mounting values of the Hartmann number M decrease the velocity distribution and increase the energy field.

Chapter 4

Magneto-micropolar nanofluid flow over a convectively heated sheet with nonlinear radiation and viscous dissipation

4.1 Introduction

In this chapter, we extend the flow model of Ramzan et al. [36] presented in the previous chapter in which the effect of micropoler fluid over a porous stretching sheet in the presence of Joule heating, mixed convection and magnetohydrodynamics with convective boundary conditions is discussed. Further, keeping in view the importance of nanofluids, their effect is also incorporated during the modeling process. The importance of thermal radiation can be seen in the processes which are performed at high temperature under isothermal and non-isothermal situations. The proper knowledge of thermal radiation is required during such processes to achieve the best quality final product. In most of the cases, a linear thermal radiation is considered, whereas for the higher temperature processes this yields a noticeable error. So a nonlinear temperature dependent thermal radiation effect

has been considered in the present chapter. At the boundary, the slip conditions are considered as discussed in Chapter 3. The nonlinar PDEs are converted into a set of ODEs by employing a proper similarity transformation. Numerical solution of these modeled ODEs are acquired by using the shooting method. The final part of chapter contains the outcomes for some physical parameters affecting the flow and heat transfer. Significance of different physical parameters on dimensionless velocity and temperature are elaborated through graphs and tables.

4.2 Problem formulation

We have consider the dimensionless steady, incompressible magneto micropolar nanofluid flow over the permeable stretching sheet with slip velocity and convective boundary condition. The geometry of the flow model is shown in Figure 4.1.

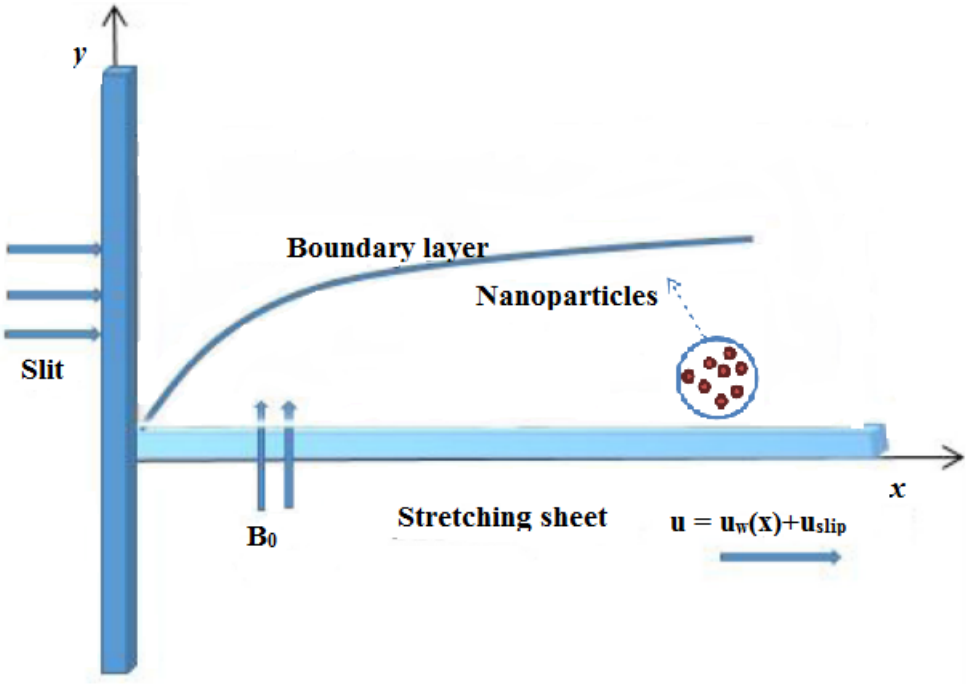

Figure 4.1: Geometry of the folw under dissection.

The associated equations for the flow model are given in (4.1)-(4.5), which under boundary layer approximation can be written as,

$$\frac{\partial u}{\partial x}+\frac{\partial v}{\partial y}=0, \tag{4.1}$$

$$u\frac{\partial u}{\partial x}+v\frac{\partial u}{\partial y}=\left(\frac{\mu+\kappa}{\rho}\right)\frac{\partial^2 u}{\partial y^2}-\frac{\kappa}{\rho}\frac{\partial N}{\partial y}+\frac{\sigma}{\rho}(E_0B_0-B_0^2u) \tag{4.2}$$

$$u\frac{\partial N}{\partial x}+v\frac{\partial N}{\partial y}=\frac{\gamma^*}{\rho j}\frac{\partial^2 N}{\partial^2 y}-\frac{\kappa}{\rho j}(2N+\frac{\partial u}{\partial y}), \tag{4.3}$$

$$\begin{aligned}u\frac{\partial T}{\partial x}+v\frac{\partial T}{\partial y}&=\frac{\kappa_1}{\rho C_p}\frac{\partial^2 T}{\partial y^2}+\frac{(uB_0-E_0)^2\,\sigma}{\rho C_p}+\frac{1}{\rho C_p}\frac{16\sigma^*}{3\kappa^*}T_\infty^*\frac{\partial^2 T}{\partial y^2}\\&+\left(\frac{\mu+\kappa}{\rho C_p}\right)\left(\frac{\partial u}{\partial y}\right)^2+\tau\left[D_B\frac{\partial T}{\partial y}\frac{\partial C}{\partial y}+\frac{D_T}{T_\infty}\left(\frac{\partial T}{\partial y}\right)^2\right],\end{aligned} \tag{4.4}$$

$$u\frac{\partial C}{\partial x}+v\frac{\partial C}{\partial y}=D_B\frac{\partial^2 C}{\partial y^2}+\frac{D_T}{T_\infty}\frac{\partial^2 T}{\partial y^2}. \tag{4.5}$$

The associated boundary conditions for the above system of equations are,

$$\left.\begin{aligned}&u=ax+\sigma^*\left[(\mu+\kappa)\frac{\partial u}{\partial y}+\kappa N\right],\quad v=v_w,\\&N=-n\frac{\partial u}{\partial y},\quad -\kappa\left(\frac{\partial T}{\partial y}\right)=h_f[T_f-T],\\&-D_B\frac{\partial C}{\partial y}=h_m(c_f-c),\qquad \text{at}\quad y=0,\\&u\to 0,\quad N\to 0,\quad T\to T_\infty,\quad c\to c_\infty,\qquad \text{as}\quad y\to\infty.\end{aligned}\right\} \tag{4.6}$$

4.3 Solution of problem

In this portion we convert the system of (4.1) - (4.5) along with the boundary conditions (4.6) into a unitless form. To find out the solution of PDEs we use the following similarity transformation.

$$\left.\begin{aligned}&\eta=\sqrt{\frac{a}{\nu}}y,\quad N=ax\sqrt{\frac{a}{\nu}}h(\eta),\quad u=\frac{\partial\psi}{\partial y},\quad v=-\frac{\partial\psi}{\partial x},\\&\psi(x,y)=\sqrt{a\nu}xf(\eta),\quad \phi(\eta)=\frac{C-C_\infty}{C_f-C_\infty},\quad and\quad \theta(\eta)=\frac{T-T_\infty}{T_f-T_\infty}.\end{aligned}\right\} \tag{4.7}$$

Here the parameters K, M, R, Ec, f_w, α, Pr, Le, Ec, Nb and Nt are the material parameter, Hartman number, radiation parameter, Eckert number, suction/injection velocity, slip parameter, Prandtl number, Lewis number, Eckert number, Brownian motion parameter and Thermophoresis parameter respectively. These quantities are formulated as follows:

$$\begin{aligned}
K &= \frac{\kappa}{\mu} \\
M^2 &= \frac{\sigma B_0^2}{\rho a} \\
f_w &= -(a\nu)^{\frac{-1}{2}} v_w \\
Pr &= \frac{\mu C_p}{\kappa} \\
\alpha &= \alpha^* \mu \sqrt{\frac{a}{\upsilon}} \\
E &= \frac{E_0}{u_w B_0} \\
R &= \frac{4\sigma^* T_\infty^3}{\kappa^* \kappa_1} \\
Le &= \frac{\alpha}{D_B} \\
Ec &= \frac{u_w^2}{C_p(T_f - T_\infty)} \\
Nb &= \frac{\tau D_B}{\nu} \frac{(\rho c)_p}{(\rho c)_f} (C_f - C_\infty) \\
Nt &= \frac{D_T (\rho c)_p}{T_\infty (\rho c)_f \nu} (T_f - T_\infty).
\end{aligned}$$

The detailed procedure for conversion of equation (4.1)-(4.3) as we have alraedy computed in chapter 3. Now the detailed procedure for conversion of equation (4.4) and (4.5) has been described in the upcomming discusion.

- $\theta(\eta) = \dfrac{T - T_\infty}{T_f - T_\infty}.$

$$\Rightarrow \quad T = (T_f - T_\infty)\theta(\eta) + T_\infty, \tag{4.8}$$

- $$\frac{\partial T}{\partial x} = 0. \tag{4.9}$$
- $$u\frac{\partial T}{\partial x} = 0. \tag{4.10}$$
- $$\frac{\partial T}{\partial y} = \theta'(\eta)\sqrt{\frac{a}{\nu}}\,(T_f - T_\infty). \tag{4.11}$$
- $$v\frac{\partial T}{\partial y} = -\theta'(\eta)f(\eta)a\,(T_f - T_\infty). \tag{4.12}$$

Using (4.10) and (4.12) the left side of (4.4) gets the following form:

$$\begin{aligned} u\frac{\partial T}{\partial x} + v\frac{\partial T}{\partial y} &= 0 - \theta'(\eta)f(\eta)a(T_f - T_\infty) \\ &= -a(T_f - T_\infty)\theta'(\eta)f(\eta). \end{aligned} \tag{4.13}$$

To convert the right side of (4.4), into dimensionless form, we proceed as follows.

- $$\frac{\partial^2 T}{\partial y^2} = \frac{a}{\nu}\,(T_f - T_\infty)\theta''(\eta).$$
- $$\frac{\kappa_1}{\rho C_p}\frac{\partial^2 T}{\partial y^2} = \frac{\kappa_1}{\rho C_p}\frac{a}{\nu}\,(T_f - T_\infty)\theta''(\eta). \tag{4.14}$$
- $$\begin{aligned} \frac{(uB_0 - E_0)^2\,\sigma}{\rho C_p} &= \frac{(u^2B_0^2 + E_0^2 - 2E_0uB_0)}{\rho C_p}\sigma \\ &= \frac{(a^2x^2(f'(\eta))^2B_0^2 + E_0^2 - 2E_0axf'(\eta)B_0)}{\rho C_p}\sigma \quad (\because u = axf'(\eta)) \\ &= (ax)^2B_0^2\frac{\left((f'(\eta))^2 + \frac{E_0^2}{(ax)^2B_0^2} - \frac{2E_0}{(ax)B_0}f'(\eta)\right)}{\rho C_p}\sigma \quad (\because u_w = ax) \\ &= u_w^2B_0^2\sigma\frac{((f'(\eta))^2 + E^2 - 2Ef'(\eta))}{\rho C_p} \qquad \left(\because E = \frac{E_0}{(ax)B_0}\right). \end{aligned} \tag{4.15}$$
- $$\frac{1}{\rho C_p}\frac{16\sigma^*}{3\kappa^*}T_\infty^*\frac{\partial^2 T}{\partial y^2} = \frac{1}{\rho C_p}\frac{16\sigma^*}{3\kappa^*}T_\infty^*\frac{a}{\nu}\theta''(\eta)\,(T_f - T_\infty)$$

$$= \frac{4\kappa_1}{3\rho C_p}\frac{4\sigma^* T_\infty^*}{\kappa_1\kappa^*}\frac{a}{\nu}\theta''(\eta)\,(T_f - T_\infty)$$

$$= \frac{4}{3}\frac{a}{\nu}\frac{\kappa_1 R}{\rho C_p}\,(T_f - T_\infty)\,\theta''(\eta). \qquad \left(\because R = \frac{4\sigma^*}{\kappa_1\kappa^*}T_\infty^*\right) \tag{4.16}$$

- $\left(\frac{\mu+\kappa}{\rho C_p}\right)\left(\frac{\partial u}{\partial y}\right)^2 = \left(\frac{\mu+\kappa}{\rho C_p}\right)\left(\frac{a^{\frac{3}{2}}x}{\sqrt{\nu}}\right)^2 (f''(\eta))^2$

$$= \left(\frac{\mu+\kappa}{\rho\nu}\right)\left(\frac{a^3x^2}{c_p}\right)(f''(\eta))^2$$

$$= \left(\frac{\mu+\kappa}{\mu}\right)\left(\frac{(ax)^2 a}{C_p}\right)(f''(\eta))^2 \quad (\because u_w = ax), \quad (\mu = \rho\nu)$$

$$= \left(\frac{\mu}{\mu} + \frac{\kappa}{\mu}\right)\left(\frac{u_w^2 a}{c_p}\right)(f''(\eta))^2$$

$$= (1+K)\left(\frac{u_w^2 a}{C_p}\right)(f''(\eta))^2 \qquad \left(\because K = \frac{\kappa}{\mu}\right)$$

$$= \left[(1+K)\left(\frac{u_w^2}{C_p(T_f - T_\infty)}\right)\left(\frac{\nu\rho C_p}{\kappa_1}\right)\right](f''(\eta))^2$$

$$\left(\frac{a\kappa_1}{\rho C_p}\right)(T_f - T_\infty)$$

$$= \left[(1+K)EcPr\,(f''(\eta))^2\right]\left(\frac{a\kappa_1}{\nu\rho C_p}\right)(T_f - T_\infty). \tag{4.17}$$

$\because \quad Ec = \frac{u_w^2}{C_p(T_f - T_\infty)}, Pr = \frac{\nu\rho C_p}{\kappa_1}$

- $\phi(\eta) = \frac{(C - C_\infty)}{(C_f - C_\infty)}.$

$\Rightarrow \phi(\eta)\,(C_f - C_\infty) = (C - C_\infty)$

$$C = \phi(\eta)\,(C_f - C_\infty) + C_\infty$$

- $$\frac{\partial C}{\partial y} = \frac{\partial}{\partial x}\left(\phi\left(\sqrt{\frac{a}{\nu}}y\right)(C_f - C_\infty) + C_\infty\right) \tag{4.18}$$

$$= \sqrt{\frac{a}{\nu}}\,(C_f - C_\infty)\,\phi'(\eta).$$

- $\tau D_B \frac{\partial T}{\partial y}\frac{\partial C}{\partial y} = \tau\left(D_B\left(\sqrt{\frac{a}{\nu}}\right)(T_f - T_\infty)\theta'(\eta)\right)\left(\sqrt{\frac{a}{\nu}}\,(C_f - C_\infty)\,\phi'(\eta)\right)$

$$= a\left[\frac{D_B}{\nu}\frac{(\rho c)_p}{(\rho c)_f}(C_f - C_\infty)\theta'(\eta)\phi'(\eta)\right](T_f - T_\infty) \quad \left(\because \tau = \frac{(\rho c)_p}{(\rho c)_f}\right)$$

$$= [N_b\theta'(\eta)\phi'(\eta)]\,(T_f - T_\infty)a. \quad \left(\because Nb = \frac{\tau D_B}{\nu}\frac{(\rho c)_p}{(\rho c)_f}(C_f - C_\infty)\right) \tag{4.19}$$

- $\tau\frac{D_T}{T_\infty}\left(\frac{\partial T}{\partial y}\right)^2 = \tau\frac{D_T}{T_\infty}\left(\left(\sqrt{\frac{a}{\nu}}\right)(T_f - T_\infty)\theta'(\eta)\right)^2$

$$= \left[\frac{D_T(\rho c)_p}{T_\infty(\rho c)_f\nu}(T_f - T_\infty)(\theta'(\eta))^2\right](T_f - T_\infty)a$$

$$= \left[N_t(\theta'(\eta))^2\right](T_f - T_\infty)a \quad \left(\because Nt = \frac{D_T(\rho c)_p}{T_\infty(\rho c)_f\nu}(T_f - T_\infty)\right)$$

$$= \left[N_t(\theta'(\eta))^2\right](T_f - T_\infty)a. \tag{4.20}$$

- $\theta(\eta) = \dfrac{T - T_\infty}{T_f - T_\infty},$

$\Rightarrow \quad T = \theta(T_f - T_\infty) + T_\infty = T_\infty\left[\left(\dfrac{T_f}{T_\infty}\right)\theta(\eta) + 1\right],$

$\Rightarrow \quad T = T_\infty\left[(Q_w - 1)\theta(\eta) + 1\right].$

- $\dfrac{\partial T}{\partial y} = T_\infty(Q_w - 1)\dfrac{\partial T}{\partial y}.$

- $q_r = -\dfrac{4\sigma^*}{3\kappa^*}\dfrac{\partial T^4}{\partial y} = -\dfrac{16\sigma^*}{3\kappa^*}T^*\dfrac{\partial T}{\partial y}$
$= -\dfrac{16\sigma^* T_\infty^*}{3\kappa^*}\left[(Q_w - 1)\theta(\eta) + 1\right]^3\dfrac{\partial T}{\partial y}.$

- $\dfrac{1}{\rho C_p}\dfrac{\partial q_r}{\partial y} = -\dfrac{16\sigma^* T^*}{3\kappa^*\rho c_p}\left[\left((Q_w - 1)\theta(\eta) + 1\right)^3\dfrac{\partial^2 T}{\partial y^2}\right]$
$- \dfrac{16\sigma^* T^*}{3\kappa^*\rho c_p}\left[\dfrac{\partial T}{\partial y}3\left((Q_w - 1)\theta(\eta) + 1\right)^2(Q_w - 1)\dfrac{\partial\theta}{\partial y}\right]$
$= -\dfrac{16\sigma^* T_\infty^*}{3\kappa^*\rho C_p}\left[\left((Q_w - 1)\theta(\eta) + 1\right)^3\dfrac{a}{\nu}(T_f - T_\infty)\theta''(\eta)\right]$
$- \dfrac{16\sigma^* T_\infty^*}{3\kappa^*\rho C_p}\left[3\left((Q_w - 1)\theta(\eta) + 1\right)^2(Q_w - 1)\right]$
$\left[\theta'(\eta)\sqrt{\dfrac{a}{\nu}}(T_f - T_\infty)\dfrac{1}{(T_f - T_\infty)}\sqrt{\dfrac{a}{\nu}}(T_f - T_\infty)\theta'(\eta)\right]$
$= -\dfrac{16\sigma^* T_\infty^*}{3\kappa^*\kappa_1}\dfrac{\kappa_1 a}{\rho C_p\nu}\left[\left((Q_w - 1)\theta(\eta) + 1\right)^3\theta''(\eta)\right]$
$- \dfrac{16\sigma^* T_\infty^*}{3\kappa^*\kappa_1}\dfrac{\kappa_1 a}{\rho C_p\nu}\left[3\left((Q_w - 1)\theta(\eta) + 1\right)^2(Q_w - 1)\theta'^2(\eta)\right](T_f - T_\infty)$
$= -\dfrac{4R_d}{3Pr}a(T_f - T_\infty)\left[\left((Q_w - 1)\theta(\eta) + 1\right)^3\theta''(\eta)\right]$
$- \dfrac{4R_d}{3Pr}a(T_f - T_\infty)\left[3\left((Q_w - 1)\theta(\eta) + 1\right)^2(Q_w - 1)\theta'^2(\eta)\right]$
$= -\dfrac{4R_d}{3Pr}\dfrac{\nu\rho C_p}{\kappa_1}\dfrac{\kappa_1}{\nu\rho C_p}a(T_f - T_\infty)\left[\left((Q_w - 1)\theta(\eta) + 1\right)^3\theta''(\eta)\right]$
$- \dfrac{4R_d}{3Pr}\dfrac{\nu\rho C_p}{\kappa_1}\dfrac{\kappa_1}{\nu\rho C_p}a(T_f - T_\infty)$
$\left[3\left((Q_w - 1)\theta(\eta) + 1\right)^2(Q_w - 1)\theta'^2(\eta)\right]$
$= -\dfrac{4R_d}{3Pr}Pr\dfrac{\kappa_1}{\nu\rho C_p}a(T_f - T_\infty)\left[\left((Q_w - 1)\theta(\eta) + 1\right)^3\theta''(\eta)\right]$
$- \dfrac{4R_d}{3Pr}Pr\dfrac{\kappa_1}{\nu\rho C_p}a(T_f - T_\infty)\left[3\left((Q_w - 1)\theta(\eta) + 1\right)^2(Q_w - 1)\theta'^2(\eta)\right]$
$= -\dfrac{4R_d}{3}\dfrac{\kappa_1}{\nu\rho C_p}a(T_f - T_\infty)\left[\left((Q_w - 1)\theta(\eta) + 1\right)^3\theta''(\eta)\right]$
$- \dfrac{4R_d}{3}\dfrac{\kappa_1}{\nu\rho C_p}a(T_f - T_\infty)\left[3\left((Q_w - 1)\theta(\eta) + 1\right)^2(Q_w - 1)\theta'^2(\eta)\right].$

Using Eqs. (4.14)-(4.20), the dimensionless form of right side (4.4) is as follows.

$$
\begin{aligned}
&\frac{\kappa_1}{\rho C_p}\frac{\partial^2 T}{\partial y^2}+\frac{\left(uB_0-E_0\right)^2\sigma}{\rho C_p}+\frac{1}{\rho C_p}\frac{16\sigma^*}{3\kappa^*}T_\infty^*\frac{\partial^2 T}{\partial y^2}+\left(\frac{\mu+\kappa}{\rho C_p}\right)\left(\frac{\partial u}{\partial y}\right)^2\\
&\quad+\tau\left[D_B\frac{\partial T}{\partial y}\frac{\partial C}{\partial y}+\frac{D_T}{T_\infty}\left(\frac{\partial T}{\partial y}\right)^2\right]\\
&=\frac{\kappa_1}{\rho C_p}\frac{a}{\nu}\left(T_f-T_\infty\right)\theta''(\eta)\\
&\quad+u_w^2B_o^2\sigma\frac{((f')^2(\eta)+E^2-2Ef'(\eta))}{\rho C_p}+\frac{4}{3}\frac{a}{\nu}\frac{\kappa_1 R}{\rho c_p}\theta''(\eta)\left(T_f-T_\infty\right)\\
&\quad+\left[(1+K)EcPr\left(f''(\eta)\right)^2\right]\left(\frac{a\kappa_1}{\rho C_p}\right)\left(T_f-T_\infty\right)\\
&\quad+\left[Nb\theta'(\eta)\phi'(\eta)\right]\left(T_f-T_\infty\right)a+\left[N_t(\theta'(\eta))^2\right]a\left(T_f-T_\infty\right)\\
&\quad-\frac{4R_d}{3}\frac{\kappa_1}{\nu\rho C_p}a(T_f-T_\infty)\left[\left((Q_w-1)\theta(\eta)+1\right)^3\theta''(\eta)\right]\\
&\quad-\frac{4R_d}{3}\frac{\kappa_1}{\nu\rho C_p}a(T_f-T_\infty)\left[3\left((Q_w-1)\theta(\eta)+1\right)^2(Q_w-1)\theta'^2(\eta)\right]\\
&=a\left(T_f-T_\infty\right)\left[\frac{\kappa_1}{\rho\nu C_p}\left(1+\frac{4R}{3}\right)\theta''(\eta)\right]\\
&\quad+a\left(T_f-T_\infty\right)\left[\left(\frac{u_w^2}{C_p\left(T_f-T_\infty\right)}\right)\left(\frac{B_0^2\sigma}{\rho a}\right)\left(f'^2(\eta)+E^2-2Ef'(\eta)\right)\right]\\
&\quad+\left[(1+K)EcPr\left(f''(\eta)\right)^2\right]\left(\frac{\kappa_1}{\nu\rho C_p}\right)a(T_f-T_\infty)\\
&\quad+\left[Nb\theta'(\eta)\phi'(\eta)\right]\left(T_f-T_\infty\right)a+\left[Nt(\theta'(\eta))^2\right]\left(T_f-T_\infty\right)a\\
&\quad-\frac{4R_d}{3}\frac{\kappa_1}{\nu\rho C_p}a(T_f-T_\infty)\left[\left((Q_w-1)\theta(\eta)+1\right)^3\theta''(\eta)\right]\\
&\quad-\frac{4R_d}{3}\frac{\kappa_1}{\nu\rho C_p}a(T_f-T_\infty)\left[3\left((Q_w-1)\theta(\eta)+1\right)^2(Q_w-1)\theta'^2(\eta)\right]\\
&=a\left(T_f-T_\infty\right)\left[\frac{\kappa_1}{\mu C_p}\left(1+\frac{4R}{3}\right)\theta''(\eta)+EcM^2\left(f'^2(\eta)+E^2-2Ef'(\eta)\right)\right]\\
&\quad+\left[(1+K)EcPr\left(f''(\eta)\right)^2\right]\left(\frac{a\kappa_1}{\nu\rho C_p}\right)\left(T_f-T_\infty\right)\\
&\quad+\left[N_b\theta'(\eta)\phi'(\eta)+N_t(\theta'(\eta))^2\right]\left(T_f-T_\infty\right)a\\
&\left(\because Ec=\frac{u_w^2}{C_p\left(T_f-T_\infty\right)},M^2=\frac{B_o^2\sigma}{\rho a}\right)\\
&\quad-\frac{4R_d}{3}\frac{\kappa_1}{\nu\rho C_p}a(T_f-T_\infty)\left[\left((Q_w-1)\theta(\eta)+1\right)^3\theta''(\eta)\right]\\
&\quad-\frac{4R_d}{3}\frac{\kappa_1}{\nu\rho C_p}a(T_f-T_\infty)\left[3\left((Q_w-1)\theta(\eta)+1\right)^2(Q_w-1)\theta'^2(\eta)\right]
\end{aligned}
$$

$$
\begin{aligned}
&= \frac{a\kappa_1}{\mu C_p}(T_f - T_\infty)\left[\left(1+\frac{4R}{3}\right)\theta''(\eta) + \frac{\mu C_p}{\kappa_1}EcM^2\left(f'^2(\eta)+E^2-2Ef'(\eta)\right)\right] \\
&+ \left[(1+K)EcPr\left(f''(\eta)\right)^2\right]\left(\frac{a\kappa_1}{\nu\rho C_p}\right)(T_f - T_\infty) \\
&+ \left[Nb\theta'(\eta)\phi'(\eta) + Nt(\theta'(\eta))^2\right]\left(\frac{\nu\rho C_p}{\kappa_1}\right)\left(\frac{\kappa_1}{\nu\rho c_p}\right)(T_f - T_\infty)a \quad \because (\mu = \rho\nu) \\
&- \frac{4R_d}{3}\frac{\kappa_1}{\nu\rho C_p}a(T_f - T_\infty)\left[\left((Q_w-1)\theta(\eta)+1\right)^3\theta''(\eta)\right] \\
&- \frac{4R_d}{3}\frac{\kappa_1}{\nu\rho C_p}a(T_f - T_\infty)\left[3\left((Q_w-1)\theta(\eta)+1\right)^2(Q_w-1)\theta'^2(\eta)\right] \\
&= \frac{a\kappa_1}{\mu C_p}(T_f - T_\infty)\left[\left(1+\frac{4R}{3}\right)\theta''(\eta) + PrEcM^2\left(f'^2(\eta)+E^2-2Ef'(\eta)\right)\right] \\
&+ \left[(1+K)EcPr\left(f''(\eta)\right)^2\right]\left(\frac{\kappa_1}{\nu\rho C_p}\right)a(T_f - T_\infty) \\
&+ \left[Nb\theta'(\eta)\phi'(\eta) + Nt(\theta'(\eta))^2\right]Pr\left(\frac{\kappa_1}{\mu_p}\right)a(T_f - T_\infty) \qquad \left(\because Pr = \frac{\mu C_p}{\kappa_1}\right) \\
&- \frac{4R_d}{3}\frac{\kappa_1}{\nu\rho C_p}a(T_f - T_\infty)\left[\left((Q_w-1)\theta(\eta)+1\right)^3\theta''(\eta)\right] \\
&- \frac{4R_d}{3}\frac{\kappa_1}{\nu\rho C_p}a(T_f - T_\infty)\left[3\left((Q_w-1)\theta(\eta)+1\right)^2(Q_w-1)\theta'^2(\eta)\right] \\
&= \frac{a\kappa_1}{\mu C_p}(T_f - T_\infty)\left[\left(1+\frac{4R}{3}\right)\theta''(\eta) + \frac{\mu c_p}{\kappa_1}E_cM^2\left(f'^2(\eta)+E^2-2Ef'(\eta)\right)\right] \\
&+ \frac{a\kappa_1}{\mu C_p}(T_f - T_\infty)\left[Nb\theta'(\eta)\phi'(\eta) + Nt(\theta'(\eta))^2\right]P_r \\
&+ \left(\frac{\kappa_1}{\mu C_p}\right)a(T_f - T_\infty)\left[(1+K)EcPr\left(f''(\eta)\right)^2\right] \\
&- \frac{4R_d}{3}\frac{\kappa_1}{\nu\rho C_p}a(T_f - T_\infty)\left[\left((Q_w-1)\theta(\eta)+1\right)^3\theta''(\eta)\right] \\
&- \frac{4R_d}{3}\frac{\kappa_1}{\nu\rho C_p}a(T_f - T_\infty)\left[3\left((Q_w-1)\theta(\eta)+1\right)^2(Q_w-1)\theta'^2(\eta)\right]. \qquad (4.21)
\end{aligned}
$$

Hence the dimensionless form of (4.4) becomes.

$$
\begin{aligned}
u\frac{\partial T}{\partial x} + v\frac{\partial T}{\partial y} &= \frac{\kappa_1}{\rho C_p}\frac{\partial^2 T}{\partial y^2} + \frac{\left(uB_0 - E_0\right)^2\sigma}{\rho C_p} + \frac{1}{\rho C_p}\frac{16\sigma^*}{3\kappa^*}T_\infty^*\frac{\partial^2 T}{\partial y^2} \\
&+ \left(\frac{\mu+\kappa}{\rho C_p}\right)\left(\frac{\partial u}{\partial y}\right)^2 + \tau\left[D_B\frac{\partial T}{\partial y}\frac{\partial C}{\partial y} + \frac{D_T}{T_\infty}\left(\frac{\partial T}{\partial y}\right)^2\right]
\end{aligned}
$$

$$
\begin{aligned}
&\Rightarrow -a(T_f - T_\infty)\theta'(\eta)f(\eta) \\
&= \frac{a\kappa_1}{\mu C_p}(T_f - T_\infty)\left[\left(1+\frac{4R}{3}\right)\theta''(\eta) + \frac{\mu C_p}{\kappa_1}E_c M^2\left(f'^2(\eta) + E^2 - 2Ef'(\eta)\right)\right] \\
&\quad + \frac{a\kappa_1}{\mu C_p}(T_f - T_\infty)\left[Nb\theta'(\eta)\phi'(\eta) + Nt(\theta'(\eta))^2\right]P_r \\
&\quad + \left(\frac{\kappa_1}{\mu C_p}\right)a(T_f - T_\infty)\left[(1+K)EcPr\left(f''(\eta)\right)^2\right] \\
&\quad - \frac{4R_d}{3}\frac{\kappa_1}{\nu\rho C_p}a(T_f - T_\infty)\left[((Q_w-1)\theta(\eta)+1)^3\theta''(\eta)\right] \\
&\quad - \frac{4R_d}{3}\frac{\kappa_1}{\nu\rho C_p}a(T_f - T_\infty)\left[3\left((Q_w-1)\theta(\eta)+1\right)^2(Q_w-1)\theta'^2(\eta)\right] \\
&\Rightarrow -\frac{\mu C_p}{\kappa_1}\theta'(\eta)f(\eta) \\
&= \left[\left(1+\frac{4R}{3}\right)\theta''(\eta) + PrEcM^2\left(f'^2(\eta) + E^2 - 2Ef'(\eta)\right)\right] \\
&\quad + \left[Nb\theta'(\eta)\phi'(\eta) + Nt(\theta'(\eta))^2\right]P_r \\
&\quad + \left[(1+K)EcPr\left(f''(\eta)\right)^2\right] - \frac{4R_d}{3}\left[((Q_w-1)\theta(\eta)+1)^3\theta''(\eta)\right] \\
&\quad - \frac{4R_d}{3}\left[3\left((Q_w-1)\theta(\eta)+1\right)^2(Q_w-1)\theta'^2(\eta)\right] \\
&\Rightarrow -P_r\theta'(\eta)f(\eta) \\
&= \left[\left(1+\frac{4R}{3}\right)\theta''(\eta) + PrEcM^2\left(f'^2(\eta) + E^2 - 2Ef'(\eta)\right)\right] \\
&\quad + \left[Nb\theta'(\eta)\phi'(\eta) + Nt(\theta'(\eta))^2\right]Pr \\
&\quad + \left[(1+K)EcPr\left(f''(\eta)\right)^2\right] - \frac{4R_d}{3}\left[((Q_w-1)\theta(\eta)+1)^3\theta''(\eta)\right] \\
&\quad - \frac{4R_d}{3}\left[3\left((Q_w-1)\theta(\eta)+1\right)^2(Q_w-1)\theta'^2(\eta)\right] \\
&\Rightarrow P_r\theta'(\eta)f(\eta) + \left[\left(1+\frac{4R}{3}\right)\theta''(\eta) + PrEcM^2\left(f'^2(\eta) + E^2 - 2Ef'(\eta)\right)\right] \\
&\quad + \left[N_b\theta'(\eta)\phi'(\eta) + Nt(\theta'(\eta))^2\right]Pr \\
&\quad + \left[(1+K)EcPr\left(f''(\eta)\right)^2\right] - \frac{4R_d}{3}\left[((Q_w-1)\theta(\eta)+1)^3\theta''(\eta)\right] \\
&\quad - \frac{4R_d}{3}\left[3\left((Q_w-1)\theta(\eta)+1\right)^2(Q_w-1)\theta'^2(\eta)\right] = 0 \\
&\theta''(\eta)\left[1+\frac{4R_d}{3}\left((Q_w-1)\theta(\eta)+1\right)^3\right] \\
&\quad + Pr\theta'(\eta)f(\eta) + PrEcM^2\left(f'^2(\eta) + E^2 - 2Ef'(\eta)\right) \\
&\quad + 4R_d\left((Q_w-1)\theta(\eta)+1\right)^2(Q_w-1)\theta'^2(\eta)\big) + (1+K)EcPr\left(f''(\eta)\right)^2 \\
&\quad + Pr\left[Nb\theta'\phi' + Nt\theta'^2\right] = 0. \qquad (4.22)
\end{aligned}
$$

Now we conclude the procedure for conversion of (4.5) into the dimensionless form.

$$\bullet \frac{\partial C}{\partial x} = 0. \tag{4.23}$$

$$\bullet\, u\frac{\partial C}{\partial x} = axf'(\eta)(0) = 0. \tag{4.24}$$

$$\begin{aligned} \bullet\, v\frac{\partial C}{\partial y} &= -\sqrt{a\nu}f(\eta)\left(\sqrt{\frac{a}{\nu}}\right)(C_f - C_\infty)\,\phi'(\eta) \\ &= -a\,(C_f - C_\infty)\,[f(\eta)\phi'(\eta)]\,. \end{aligned} \tag{4.25}$$

Using (4.24) and (4.25), the left side of (4.5) gets the following form:

$$\begin{aligned} u\frac{\partial C}{\partial x} + v\frac{\partial C}{\partial y} &= 0 - a\,(C_f - C_\infty)\,[f(\eta)\phi'(\eta)]\,, \\ &= -a\,(C_f - C_\infty)\,[f(\eta)\phi'(\eta)]\,. \end{aligned} \tag{4.26}$$

To convert the right side of (4.5) into dimensionless form we proceed as follows.

$$\bullet \quad \frac{\partial^2 C}{\partial y^2} = \frac{a}{\nu}\,(C_f - C_\infty)\,\phi''(\eta). \tag{4.27}$$

$$\bullet \quad \frac{\partial^2 T}{\partial y^2} = \frac{a}{\nu}\,(C_f - C_\infty)\,\theta''(\eta). \tag{4.28}$$

$$\bullet\, D_B\frac{\partial^2 C}{\partial y^2} = D_B\frac{a}{\nu}\,(C_f - C_\infty)\,\phi''(\eta). \tag{4.29}$$

$$\bullet\, D_T\frac{\partial^2 T}{\partial y^2} = D_T\frac{a}{\nu}\,(C_f - C_\infty)\,\theta''(\eta) \tag{4.30}$$

$$\bullet \quad Nt = \frac{D_T(\rho c)_p(T_f - T_\infty)}{(\rho c)_f T_\infty \nu}. \tag{4.31}$$

$$\bullet \quad Nb = \frac{(\rho c)_p D_B(C_f - C_\infty)}{(\rho c)_f \nu}. \tag{4.32}$$

Using (4.27) - (4.32), the dimensionless form of right side of (4.5) is as follows.

$$
\begin{aligned}
& D_B \frac{\partial^2 C}{\partial y^2} + \frac{D_T}{T_\infty} \frac{\partial^2 T}{\partial y^2} \\
& = D_B \frac{a}{\nu} (C_f - C_\infty) \phi''(\eta) + \frac{D_T}{T_\infty} \frac{a}{\nu} (T_f - T_\infty) \theta''(\eta) \\
& = D_B \frac{a}{\nu} (C_f - C_\infty) \left[\phi''(\eta) + \frac{D_T}{T_\infty} \frac{(T_f - T_\infty)}{D_B (C_f - C_\infty)} \theta''(\eta) \right] \\
& = D_B \frac{a}{\nu} (C_f - C_\infty) \left[\phi''(\eta) + \frac{D_T}{T_\infty} \frac{(T_f - T_\infty) (\rho c)_p (\rho c)_f}{D_B (C_f - C_\infty) (\rho c)_p (\rho c)_f} \theta''(\eta) \right] \\
& = D_B \frac{a}{\nu} (C_f - C_\infty) \left[\phi''(\eta) + \frac{D_T (\rho c)_p (T_f - T_\infty)}{T_\infty \nu (\rho c)_f} \frac{1}{\frac{(\rho c)_p D_B (C_f - C_\infty)}{(\rho c)_f \nu}} \theta''(\eta) \right] \\
& = D_B \frac{a}{\nu} (C_f - C_\infty) \left[\phi''(\eta) + \frac{Nt}{Nb} \theta''(\eta) \right]. \qquad (4.33)
\end{aligned}
$$

Therefore the dimensionless form of (4.5) becomes:

$$
\begin{aligned}
& u \frac{\partial C}{\partial x} + v \frac{\partial C}{\partial y} = D_B \frac{\partial^2 C}{\partial y^2} + \frac{D_T}{T_\infty} \frac{\partial^2 T}{\partial y^2} \\
& \Rightarrow -a (C_f - C_\infty) [f(\eta) \phi'(\eta)] = D_B \frac{a}{\nu} (C_f - C_\infty) \left[\phi''(\eta) + \frac{Nt}{Nb} \theta''(\eta) \right] \\
& \Rightarrow - [f(\eta) \phi'(\eta)] = D_B \frac{1}{\nu} \left[\phi''(\eta) + \frac{Nt}{Nb} \theta''(\eta) \right] \\
& \Rightarrow - \frac{\nu}{D_B} [f(\eta) \phi'(\eta)] = \left[\phi''(\eta) + \frac{Nt}{Nb} \theta''(\eta) \right] \\
& \Rightarrow - \left(\frac{\nu}{\alpha} \right) \left(\frac{\alpha}{D_B} \right) [f(\eta) \phi'(\eta)] = \left[\phi''(\eta) + \frac{Nt}{Nb} \theta''(\eta) \right] \qquad \left(\because Le = \left(\frac{\alpha}{D_B} \right) \right) \\
& \Rightarrow -PrLe [f(\eta) \phi'(\eta)] = \left[\phi''(\eta) + \frac{Nt}{Nb} \theta''(\eta) \right] \qquad \left(\because Pr = \left(\frac{\nu}{\alpha} \right) \right) \\
& \Rightarrow \phi'' + PrLef(\eta) \phi' + \frac{Nt}{Nb} \theta'' = 0. \qquad (4.34)
\end{aligned}
$$

Rewriting the converted ODEs together,

$$(1+K)f''' + ff'' - f'^2 + Kh' - M^2 f' + M^2 E = 0, \tag{4.35}$$

$$\left(1+\frac{K}{2}\right)h'' + fh' - f'h' - K(2h+f'') = 0, \tag{4.36}$$

$$\theta''\left[1+\frac{4}{3}R_d\left((Q_w-1)\theta+1\right)^3\right] + P_r f\theta' + M^2 EcPr\left[f'^2 + E^2 - 2Ef'\right]$$
$$+ 4R_d((Q_w-1)\theta+1)^2((Q_w-1)\theta'^2) + (1+K)EcPrf''^2$$
$$+ Pr(Nb\theta'\phi' + Nt\theta'^2) = 0, \tag{4.37}$$

$$\phi''(\eta) + PrLef\phi' + \frac{Nt}{Nb}\theta'' = 0. \tag{4.38}$$

The BCs are of the form,

$$\begin{aligned}
\bullet \qquad v &= \nu_w, \\
\Rightarrow -\sqrt{a}\nu f(\eta) &= \nu_w \\
\Rightarrow \qquad f(\eta) &= -\frac{\nu_w}{\sqrt{a}\nu} \\
\Rightarrow \qquad f(\eta) &= -(a\nu)^{-\frac{1}{2}}\nu_w \\
\Rightarrow \qquad f(\eta) &= f_w. \qquad \left(\because f_w = -(a\nu)^{-\frac{1}{2}}\nu_w\right) \\
\bullet \qquad N &= -n\frac{\partial u}{\partial y} \\
\Rightarrow ax\sqrt{\frac{a}{\nu}}h(\eta) &= -n\frac{a^{\frac{3}{2}}}{\sqrt{\nu}}xf''(\eta) \\
\Rightarrow \qquad h(\eta) &= -nf''(\eta). \\
\bullet \qquad u &= ax + \alpha^*\left[(\mu+\kappa)\frac{\partial u}{\partial y} + \kappa N\right] \\
\Rightarrow \qquad axf'(\eta) &= ax + \alpha^*\left[(\mu+\kappa)\frac{a^{\frac{3}{2}}}{\sqrt{\nu}}xf''(\eta) + \kappa ax\sqrt{\frac{a}{\nu}}h(\eta)\right] \\
\Rightarrow \qquad f'(\eta) &= 1 + \alpha^*\left[(\mu+\kappa)\sqrt{\frac{a}{\nu}}f''(\eta) + \kappa\sqrt{\frac{a}{\nu}}h(\eta)\right] \\
\Rightarrow \qquad f'(\eta) &= 1 + \alpha^*\mu\sqrt{\frac{a}{\nu}}f''(\eta) + \alpha^*\kappa\sqrt{\frac{a}{\nu}}f''(\eta) + \alpha^*\kappa\sqrt{\frac{a}{\nu}}h(\eta) \\
\Rightarrow \qquad f'(\eta) &= 1 + \alpha f''(\eta) + \alpha K f''(\eta) + \alpha K h(\eta) \qquad \left(\because K = \frac{\kappa}{\mu}, \alpha = \alpha^*\mu\sqrt{\frac{a}{\nu}}\right) \\
\Rightarrow \qquad f'(\eta) &= 1 + \alpha(1+K)f''(\eta) - \alpha K n f''(\eta) \quad (\because h(\eta) = -nf''(\eta))
\end{aligned}$$

$$
\begin{aligned}
\Rightarrow \qquad f'(\eta) &= 1+\alpha(1+K-Kn)f''(\eta)\\
\Rightarrow \qquad f'(\eta) &= 1+\alpha\left(1+K(1-n)\right)f''(\eta).\\
\bullet \quad h_t\left[T_f-T\right] &= -\kappa\frac{\partial T}{\partial y}\\
\Rightarrow \quad h_t\left[T_f-T\right] &= -\kappa\left[\theta'(\eta)\sqrt{\frac{a}{\nu}}(T_f-T_\infty)\right]\\
\Rightarrow \qquad \theta'(\eta) &= -\frac{h_t\left(T_f-T\right)}{\sqrt{\frac{a}{\nu}}(T_f-T_\infty)}\\
\Rightarrow \qquad \theta'(\eta) &= -\frac{h_f}{\kappa}\sqrt{\frac{a}{\nu}}\left[T_f-\theta(\eta)\left(T_f-T_\infty\right)-T_\infty\right]\\
\Rightarrow \qquad \theta'(\eta) &= -\gamma\left(1-\theta(\eta)\right). \qquad \left(\because \gamma=\frac{h}{\kappa\sqrt{\frac{a}{\nu}}}\right)\\
\bullet \qquad u &= axf'(\eta), \qquad u\to 0,\ as\ y\to\infty\\
\Rightarrow \quad axf'(\infty) &= 0\\
\Rightarrow \qquad f'(\infty) &= 0.\\
\bullet \qquad N &= ax\sqrt{\frac{a}{\nu}}h(\eta), \qquad N\to 0,\ as\ y\to\infty\\
\Rightarrow \quad ax\sqrt{\frac{a}{\nu}}h(\eta) &= 0\\
\Rightarrow \qquad h(\infty) &= 0.\\
\bullet \qquad \theta(\eta) &= \frac{T-T_\infty}{T_f-T_\infty}, \qquad T\to T_\infty\ as\ y\to\infty\\
\Rightarrow \qquad \theta(\infty) &= 0.\\
\Rightarrow \qquad \theta(\infty) &= 0.\\
\bullet \qquad -D_B\frac{\partial C}{\partial y} &= h_m\left(C_f-C_\infty\right)\\
\Rightarrow h_m\left(C_f-C_\infty\right) &= -D_B\left[\phi'(\eta)\left(C_f-C_\infty\right)\sqrt{\frac{a}{\nu}}\right]\\
\Rightarrow \qquad \phi'(\eta) &= -\frac{h_m\left(C_f-C\right)}{D_B(C_f-C_\infty)\sqrt{\frac{a}{\nu}}}\\
\Rightarrow \qquad \phi'(\eta) &= -\frac{h_m}{D_B}\sqrt{\frac{a}{\nu}}\frac{C_f-\phi(C_f-C_\infty)-C_\infty}{C_f-C_\infty}\\
\Rightarrow \qquad \phi'(\eta) &= -\frac{h_m}{D_B}\sqrt{\frac{a}{\nu}}\left(1-\phi(\eta)\right)\\
\Rightarrow \qquad \phi'(\eta) &= -\gamma_2(1-\phi(\eta)).
\end{aligned}
$$

Rewriting the converted ODEs together,

$$\left.\begin{aligned} &f(\eta) = f_w, \qquad f'(\eta) = 1 + \alpha(1 + K(1-n))f''(\eta), \\ &h(\eta) = -nf''(\eta), \qquad \theta'(\eta) = -\gamma(1-\theta(\eta)), \\ &\phi'(\eta) = -\gamma_2(1-\phi(\eta)), \qquad \text{at} \;\; \eta = 0, \\ &f'(\eta) = 0, \quad h(\eta) = 0, \quad \theta(\eta) = 0, \quad \phi(\eta) = 0, \quad \text{at} \quad \eta \to \infty. \end{aligned}\right\} \tag{4.39}$$

The Nusselt number and the local skin friction are given as

$$C_{fx} = \frac{2\tau_w}{\rho(ax)^2}, \tag{4.40}$$

$$Nu_x = \frac{xq_w}{\kappa(T_f - T_\infty)}. \tag{4.41}$$

where τ_w and q_w are given by

$$\tau_w = \left((\mu + \kappa)\frac{\partial u}{\partial y} + \kappa N\right)_{y=0}, \tag{4.42}$$

$$q_w = -\kappa_1 \left(\frac{\partial T}{\partial y}\right)_{y=0}. \tag{4.43}$$

The dimensionless form of the above quantities becomes

$$\frac{1}{2}C_{fx}Re_x^{\frac{1}{2}} = (1 + (1-n)K)f''(0), \tag{4.44}$$

$$NuRe_x{}^{-1/2}x = -\frac{1}{3}[3 + 4R_d\left((Q_w - 1)\,\theta(0) + 1\right)^3]\theta'(0). \tag{4.45}$$

Where the local Reynolds number is defined as,

$$Re_x = ux/v. \tag{4.46}$$

The Shewood number is given by

$$Sh_x(Re_x)^{-1/2} = -\phi'(0) \tag{4.47}$$

4.4 Solution methodology

The analytic solution of the boundary value problem (4.35) - (6.39) cannot be found because these equations are non linear and coupled. So, we use a numerical technique, i.e., the shooting scheme with Runge-Kutta mechanism of fourth order. In order to sorted out the system of ordinary differential Eqs. (4.35) - (6.38), with the boundary conditions (4.39), using the shooting method, we have to first change over these expressions into an arrangement of first order differential equations. Let us use the following notations.

$$\left.\begin{aligned} f = y_1, \quad f' = y_2, \quad f'' = y_3, \\ h = y_4, \quad h' = y_5, \\ \theta = y_6, \quad \theta' = y_7, \\ \phi = y_8, \quad \phi' = y_9. \end{aligned}\right\} \tag{4.48}$$

The system of equation along with the boundary conditions converted into a set of seven first ODEs.

$$\left.\begin{aligned}
y_1' &= y_2,\\
y_2' &= y_3,\\
y_4' &= y_5,\\
y_3' &= \frac{1}{(1+K)}\left(y_2^2 - y_1y_3 - Ky_5 + M^2y_2 - M^2E\right),\\
y_5' &= \frac{2}{(2+K)}\left(y_2y_4 + K\left(2y_4 + y_3\right) - y_1y_5\right),\\
y_6' &= y_7,\\
y_7' &= \frac{1}{\left[1+\frac{4}{3}R_d\left((Q_w-1)\theta+1\right)^3\right]}\begin{bmatrix} -M^2EcPr\left(y_2^2+E^2-2Ey_2\right) - \\ 4R_d\left((Q_w-1)y_6+1\right)^2(Q_w-1)y_7^2 \\ -(1+K)EcPry_3^2 - Pry_1y_7 \\ -P_r\left(Nby_7y_9 + Nty_7^2\right), \end{bmatrix},\\
y_8' &= y_9,\\
y_9' &= -PrLey_1y_9 - \frac{Nt}{Nb}y_7'.
\end{aligned}\right\} \tag{4.49}$$

$$\left.\begin{aligned}
&y_1(0) = f_w, \quad y_2(0) = 1+\alpha(1+K(1-n))s, \quad y_3(0) = s, \quad y_4(0) = -ns,\\
&y_5(0) = t, \quad y_6(0) = u, \quad y_7(0) = -\gamma_1(1-u), \quad y_8(0) = v, \quad y_9(0) = -\gamma_2(1-v)
\end{aligned}\right\} \tag{4.50}$$

In the equations (4.50) the missing initial conditions $y_3(0)$, $y_5(0)$ and $y_6(0)$ are to be chosen such that

$$\left.\begin{aligned}
y_2(\eta_\infty, s, t, u, v) &= 0,\\
y_4(\eta_\infty, s, t, u, v) &= 0,\\
y_6(\eta_\infty, s, t, u, v) &= 0,\\
y_8(\eta_\infty, s, t, u, v) &= 0.
\end{aligned}\right\} \tag{4.51}$$

To solve the system of equations (4.51), we use the Newton's method which has the following iterative scheme

$$\begin{pmatrix} s^{(n+1)} \\ t^{(n+1)} \\ u^{(n+1)} \\ v^{(n+1)} \end{pmatrix} = \begin{pmatrix} s^{(n)} \\ t^{(n)} \\ u^{(n)} \\ v^{(n)} \end{pmatrix} - \begin{pmatrix} \frac{\partial y_2}{\partial s} & \frac{\partial y_2}{\partial t} & \frac{\partial y_2}{\partial u} & \frac{\partial y_2}{\partial v} \\ \frac{\partial y_4}{\partial s} & \frac{\partial y_4}{\partial t} & \frac{\partial y_4}{\partial u} & \frac{\partial y_4}{\partial v} \\ \frac{\partial y_6}{\partial s} & \frac{\partial y_6}{\partial t} & \frac{\partial y_6}{\partial u} & \frac{\partial y_6}{\partial v} \\ \frac{\partial y_8}{\partial s} & \frac{\partial y_8}{\partial t} & \frac{\partial y_8}{\partial u} & \frac{\partial y_8}{\partial v} \end{pmatrix}^{-1}_{(\eta_\infty, s^{(n)}, t^{(n)}, u^{(n)})} \begin{pmatrix} y_2^{(n)} \\ y_4^{(n)} \\ y_6^{(n)} \\ y_8^{(n)} \end{pmatrix}_{(\eta_\infty, s^{(n)}, t^{(n)}, u^{(n)}, v^{(n)})}$$

Let us now use the following notations:

$$\left.\begin{array}{llll} \frac{\partial y_1}{\partial s} = y_{10}, & \frac{\partial y_2}{\partial s} = y_{11}, \ldots & \frac{\partial y_9}{\partial s} = y_{18}, \\ \frac{\partial y_1}{\partial t} = y_{19}, & \frac{\partial y_2}{\partial t} = y_{20}, \ldots & \frac{\partial y_9}{\partial t} = y_{27}, \\ \frac{\partial y_1}{\partial u} = y_{28}, & \frac{\partial y_2}{\partial u} = y_{29}, \ldots & \frac{\partial y_9}{\partial u} = y_{36}, \\ \frac{\partial y_1}{\partial v} = y_{37}, & \frac{\partial y_2}{\partial v} = y_{38}, \ldots & \frac{\partial y_9}{\partial v} = y_{45}. \end{array}\right\} \tag{4.52}$$

With these new notation, the Newton's iterative scheme get the following form.

$$\begin{pmatrix} s^{(n+1)} \\ t^{(n+1)} \\ u^{(n+1)} \\ v^{(n+1)} \end{pmatrix} = \begin{pmatrix} s^{(n)} \\ t^{(n)} \\ u^{(n)} \\ v^{(n)} \end{pmatrix} - \begin{pmatrix} y_9 & y_{20} & y_{29} & y_{38} \\ y_{13} & y_{22} & y_{31} & y_{40} \\ y_{15} & y_{24} & y_{33} & y_{42} \\ y_{17} & y_{26} & y_{35} & y_{44} \end{pmatrix}^{-1}_{(\eta_\infty, s^{(n)}, t^{(n)}, u^{(n)}, v^{(n)})} \begin{pmatrix} y_2^{(n)} \\ y_4^{(n)} \\ y_6^{(n)} \\ y_8^{(n)} \end{pmatrix}_{(\eta_\infty, s^{(n)}, t^{(n)}, u^{(n)}, v^{(n)})}$$

For the execution of the above iterative scheme, we differentiate equations (4.52) w.r.t each variable s, t, u and v to have another IVP consisting of system of thirty seven ODEs. Rewriting all the fourty five ODEs together along with the corresponding ICs the following IVP.

$$y_1' = y_2,$$

$$y_2' = y_3,$$

$$y_4' = y_5,$$

$$y_3' = \frac{1}{(1+K)}\left(y_2^2 - y_1 y_3 - K y_5 + M^2 y_2 - M^2 E\right),$$

$$y_5' = \frac{2}{(2+K)}\left(y_2 y_4 + K\left(2y_4 + y_3\right) - y_1 y_5\right),$$

$$y_6' = y_7,$$

$$y_7' = \frac{1}{\left[1 + \frac{4}{3}R_d\left((Q_w-1)\theta + 1\right)^3\right]}\begin{bmatrix} -M^2 E_c P_r\left(y_2^2 + E^2 - 2Ey_2\right) - \\ 4R_d\left((Q_w-1)y_6 + 1\right)^2 (Q_w - 1) y_7^2 \\ -(1+K)EcPr y_3^2 - Pr y_1 y_7 \\ -P_r\left(Nb y_7 y_9 + Nt y_7^2\right), \end{bmatrix},$$

$$y_8' = y_9,$$

$$y_9' = -PrLe y_1 y_9 - \frac{Nt}{Nb} y_7',$$

$$y_{10}' = y_{11},$$

$$y_{11}' = y_{12},$$

$$y_{12}' = \frac{1}{(1+K)}\left(-y_1 y_{12} - y_{10} y_3 + M^2 y_{11} + 2y_2 y_{11} - K y_{14} - M^2 E\right),$$

$$y_{13}' = y_{14},$$

$$y_{14}' = \frac{2}{(2+K)}\left(y_2 y_{13} + y_4 y_{11} - y_1 y_{14} - y_{10} y_5 + K\left(2y_{13} + y_{12}\right)\right),$$

$$y_{15}' = y_{16},$$

$$y_{16}' = \frac{[-4R_d((Q_w-1)y_6+1)^2(Q_w-1)y_{15}]}{\left[1 + \frac{4}{3}R_d\left((Q_w-1)y_6 + 1\right)^3\right]}$$
$$\begin{bmatrix} [y_7' + [-Pr y_1 y_{16} - Pr y_7 y_{10} \\ -M^2 EcPr\left(2y_2 y_{11} + E^2 - 2Ey_{11}\right) \\ -8R_d\left((Q_w-1)y_6 + 1\right)(Q_w - 1) y_{15} (Q_w-1) y_7^2 \\ -8R_d\left((Q_w-1)y_6 + 1\right)^2 (Q_w - 1)\, y_7 y_{16} \\ -2(1+K)EcPr y_3 y_{12} \\ -P_r\left(Nb y_7 y_9 + Nb y_9 y_{16}\right) + 2Nt y_7 y_{16}] \end{bmatrix},$$

$$y_{17}' = y_{18},$$

$$y_{18}' = -PrLe(y_1 y_{18} + y_9 y_{10}) - \frac{Nt}{Nb} y_{16}',$$

$$y'_{19} = y_{20},$$

$$y'_{20} = y_{21},$$

$$y'_{21} = \frac{1}{(1+K)}\left(-y_1y_{21} - y_3y_{19} + M^2y_{20} + 2y_2y_{20} - Ky_{23} - M^2E\right),$$

$$y'_{22} = y_{23},$$

$$y'_{23} = \frac{2}{(2+K)}\left(y_2y_{22} + y_4y_{20} - y_1y_{23} - y_5y_{19} + K\left(2y_{22} + y_{21}\right)\right),$$

$$y'_{24} = y_{25},$$

$$y'_{25} = \frac{[-4R_d((Q_w-1)y_6+1)^2(Q_w-1)y_{24}]}{\left[1+\frac{4}{3}R_d\left((Q_w-1)y_6+1\right)^3\right]}$$

$$\begin{bmatrix} [y'_7 + [-Pry_1y_{25} - Pry_7y_{19} \\ -M^2EcPr\left(2y_2y_{20} + E^2 - 2Ey_{20}\right) \\ -8R_d\left((Q_w-1)y_6+1\right)(Q_w-1)y_{24}(Q_w-1)y_7^2 \\ -8R_d\left((Q_w-1)y_6+1\right)^2(Q_w-1)\,y_7y_{25} \\ -2(1+K)E_cP_ry_3y_{21} \\ -P_r\left(Nby_7y_{27} + Nby_9y_{25}\right) + 2Nty_7y_{25}] \end{bmatrix},$$

$$y'_{26} = y_{27},$$

$$y'_{27} = -PrLe(y_1y_{27} + y_9y_{19}) - \frac{Nt}{Nb}y'_{25},$$

$$y'_{28} = y_{29},$$

$$y'_{29} = y_{30},$$

$$y'_{30} = \frac{1}{(1+K)}\left(-y_1y_{30} - y_3y_{28} + M^2y_{29} + 2y_2y_{29} - Ky_{32} - M^2E\right),$$

$$y'_{31} = y_{32},$$

$$y'_{32} = \frac{2}{(2+K)}\left(y_2y_{31} + y_4y_{29} - y_1y_{32} - y_5y_{28} + K\left(2y_{31} + y_{30}\right)\right),$$

$$y'_{33} = y_{34},$$

$$y'_{34} = \frac{[-4R_d((Q_w-1)y_6+1)^2(Q_w-1)y_{33}]}{\left[1+\frac{4}{3}R_d\left((Q_w-1)y_6+1\right)^3\right]}$$

$$\begin{bmatrix} [y'_7 + [-P_ry_1y_{34} - P_ry_7y_{28} \\ -M^2EcPr\left(2y_2y_{29} + E^2 - 2Ey_{29}\right) \\ -8R_d\left((Q_w-1)y_6+1\right)(Q_w-1)y_{33}(Q_w-1)y_7^2 \\ -8R_d\left((Q_w-1)y_6+1\right)^2(Q_w-1)\,y_7y_{34} \\ -2(1+K)E_cPry_3y_{30} \\ -P_r\left(Nby_7y_{36} + Nby_9y_{34}\right) + 2N_ty_7y_{34}] \end{bmatrix},$$

$$
\begin{aligned}
y'_{35} &= y_{36},\\
y'_{36} &= -PrLe(y_1y_{36} + y_9y_{28}) - \frac{Nt}{Nb}y'_{34},\\
y'_{37} &= y_{38},\\
y'_{38} &= y_{39},\\
y'_{39} &= \frac{1}{(1+K)}\left(-y_1y_{39} - y_3y_{37} + M^2y_{38} + 2y_2y_{38} - Ky_{41} - M^2E\right),\\
y'_{40} &= y_{41},\\
y'_{41} &= \frac{2}{(2+K)}\left(y_2y_{40} + y_4y_{38} - y_1y_{41} - y_5y_{37} + K\left(2y_{40} + y_{39}\right)\right),\\
y'_{42} &= y_{43},\\
y'_{43} &= \frac{[-4R_d((Q_w-1)y_6+1)^2(Q_w-1)y_{42}]}{\left[1+\frac{4}{3}R_d\left((Q_w-1)y_6+1\right)^3\right]}\\
&\quad\begin{bmatrix}
[y'_7 + [-P_ry_1y_{43} - P_ry_7y_{37}\\
-M^2EcPr\left(2y_2y_{38} + E^2 - 2Ey_{38}\right)\\
-8R_d\left((Q_w-1)y_6+1\right)(Q_w-1)y_{42}(Q_w-1)y_7^2\\
-8R_d\left((Q_w-1)y_6+1\right)^2(Q_w-1)\,y_7y_{43}\\
-2(1+K)EcPry_3y_{39}\\
-Pr\left(Nby_7y_{45} + Nby_9y_{43}\right) + 2Nty_7y_{43}]
\end{bmatrix},\\
y'_{44} &= y_{45},\\
y'_{45} &= -PrLr(y_1y_{45} + y_9y_{37}) - \frac{Nt}{Nb}y'_{43}.
\end{aligned}
$$

$$y_1(0) = f_w, \quad y_2(0) = 1 + \alpha(1 + K(1-n))s, \quad y_3(0) = s, \quad y_4(0) = -ns,$$
$$y_5(0) = t, \quad y_6(0) = u, \quad y_7(0) = -\gamma_1(1-u), \quad y_8(0) = v, \quad y_9(0) = -\gamma_2(1-v),$$
$$y_{10}(0) = 0, \quad y_{11}(0) = \alpha(1 + K(1-n)), \quad y_{12}(0) = 1, \quad y_{13}(0) = -n,$$
$$y_{14}(0) = 0, \quad y_{15}(0) = 0, \quad y_{16}(0) = 0, \quad y_{17}(0) = 0, \quad y_{18}(0) = 0,$$
$$y_{19}(0) = 0, \quad y_{20}(0) = 0, \quad y_{21}(0) = 0, \quad y_{22}(0) = 0,$$
$$y_{23}(0) = 1, \quad y_{24}(0) = 0, \quad y_{25}(0) = 0, \quad y_{26}(0) = 0, \quad y_{27}(0) = 0,$$
$$y_{28}(0) = 0, \quad y_{29}(0) = 0, \quad y_{30}(0) = 0, \quad y_{31}(0) = 0,$$
$$y_{32}(0) = 0, \quad y_{33}(0) = 1, \quad y_{34}(0) = \gamma_1, \quad y_{35}(0) = 0,$$
$$y_{36}(0) = 0, \quad y_{37}(0) = 0, \quad y_{38}(0) = 0, \quad y_{39}(0) = 0,$$
$$y_{40}(0) = 0, \quad y_{41}(0) = 0, \quad y_{42}(0) = 0, \quad y_{43}(0) = 0, \quad y_{44}(0) = 1, \quad y_{45}(0) = \gamma_2.$$

The shooting method requires the initial guess for $y_3(0)$, $y_5(0)$, $y_6(0)$ and $y_8(0)$, and by using Newton's procedure we can change each guess untill we attain an approximate result for the given problem. To check accuracy of the obtained numerical results by shooting method we compare them by the numerical results acquired by Matlab bvp4c solver and found them in excellent agreement.

4.5 Results and discussion

This section analyze the effect of different parameters, Ec, α, M, K, Le, R, Nb, Nt, Pr and Q_w (i.e., Eckert number, slip parameter, Hartman number, material parameter, Lewis number, Radiation parameter, Brownian movement parameter, Thermophoresis parameter, Prandtl number and Temperature proportion ratio parameter separately.) on dimensionless velocity, dimensionless energy, dimensionless microrotation and dimensionless concentration profiles.

4.5.1 Impact of Eckert number on the unitless concentration profile and unitless energy profile

Figure. 4.2 display the influence of Eckert number Ec on concentration profile. It is observe that the concentration of the fluid increase near the plate. However it diminishes away from the surface as the value of Eckert number is enhanced. Figure. 4.3 shows the effect of Eckert number Ec on the energy profile. Energy profile increases when increase Eckert number Ec.

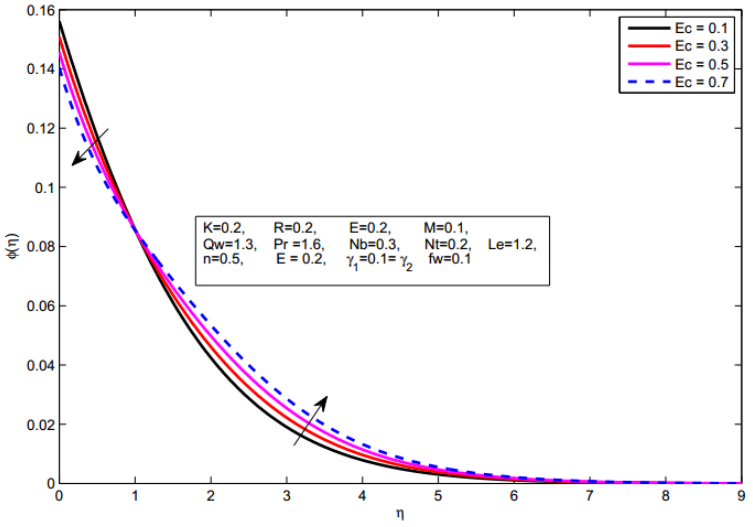

Figure 4.2: Impact of Ec on the unitless concentration $\phi(\eta)$

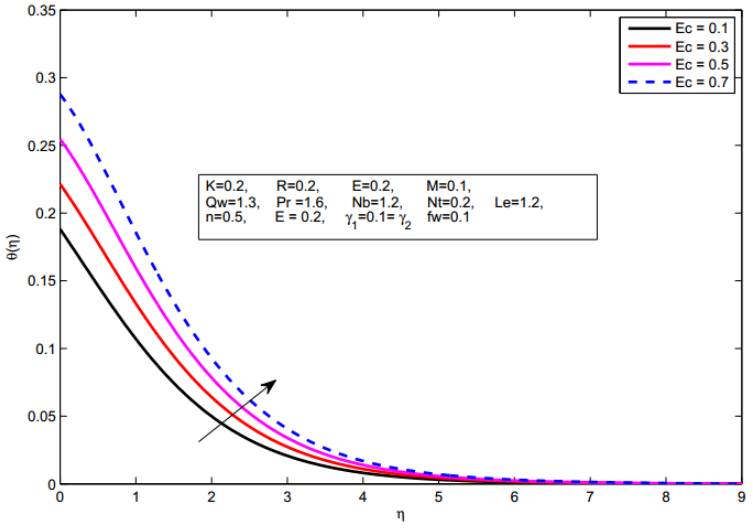

Figure 4.3: Impact of Ec on the unitless energy $\theta(\eta)$

4.5.2 Impact of slip parameter on the unitless Concentration profile and unitless energy profile

Figures. 4.4 and 4.5 illustrate the variations of slip parameter α on the concentration profile $\phi(\eta)$ and dimensionless energy profile $\theta(\eta)$ respectively. It is noted that $\phi(\eta)$ and $\theta(\eta)$ has direct relation with α. Apparently, as α mounts the lateral surface starts moving in y-direction and as a result both the Concentration profile $\phi(\eta)$ and energy profile $\theta(\eta)$ are increased.

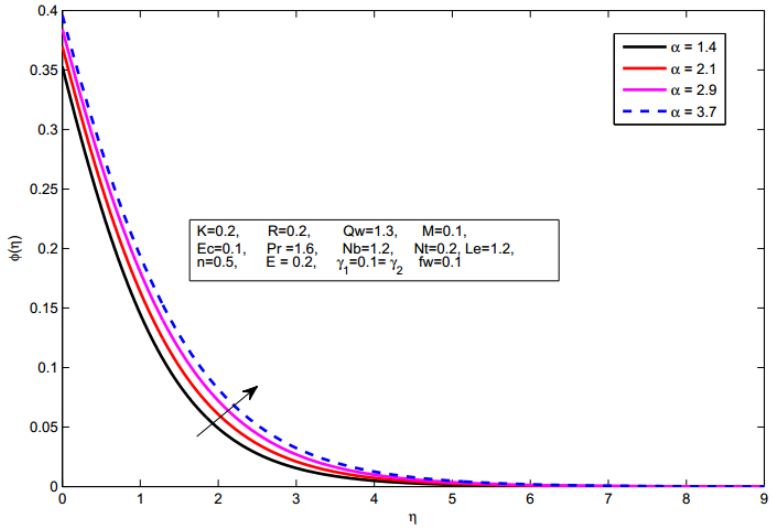

Figure 4.4: Impact of α on the unitless concentration $\phi(\eta)$

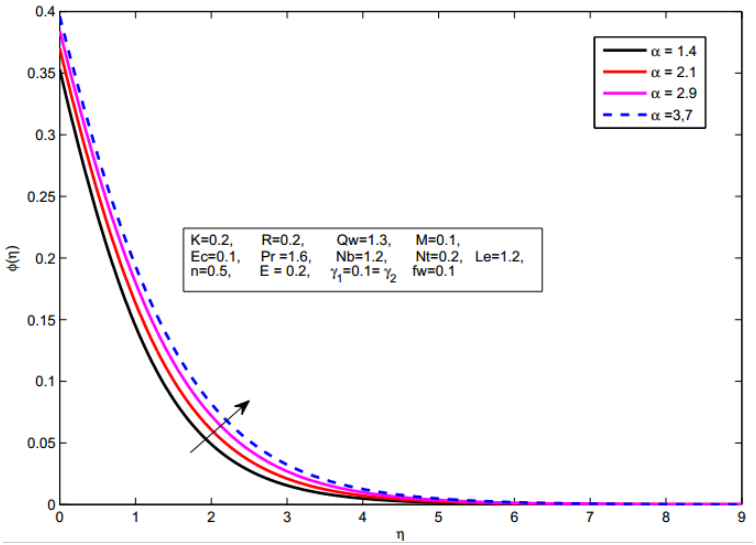

Figure 4.5: Impact of α on the unitless energy $\theta(\eta)$

4.5.3 Impact of Hartman number on unitless velocity, unitless temperature and unitless concentration

Figure. 4.6, Figure. 4.7 and Figure. 4.8 shows the variations in the velocity profile $f'(\eta)$, energy profile $\theta(\eta)$ and concentration profile $\phi(\eta)$ for different estimations of Hartman number M. It is analyzed that the temperature profile $\theta(\eta)$, concentration profile $\phi(\eta)$ and thermal boundary layer thickens are increasing functions of Hartman number, however on the opposite side velocity profile $f'(\eta)$ decreases when we increase Hartman number M.

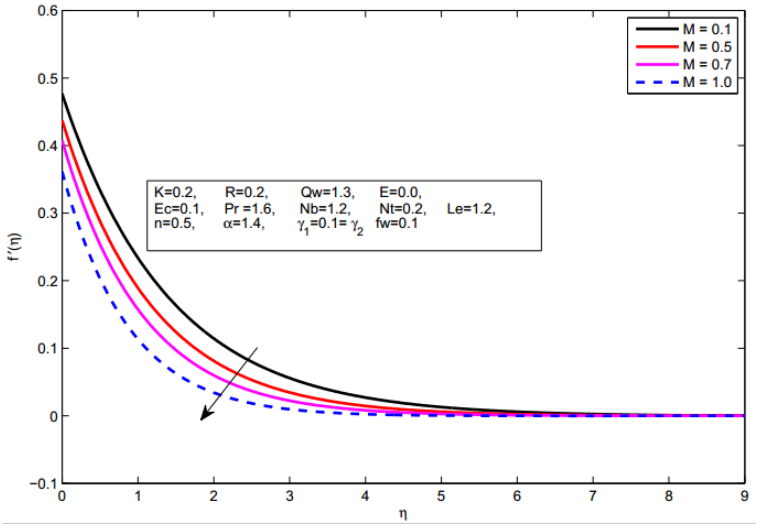

Figure 4.6: Impact of M on the unitless velocity $f'(\eta)$

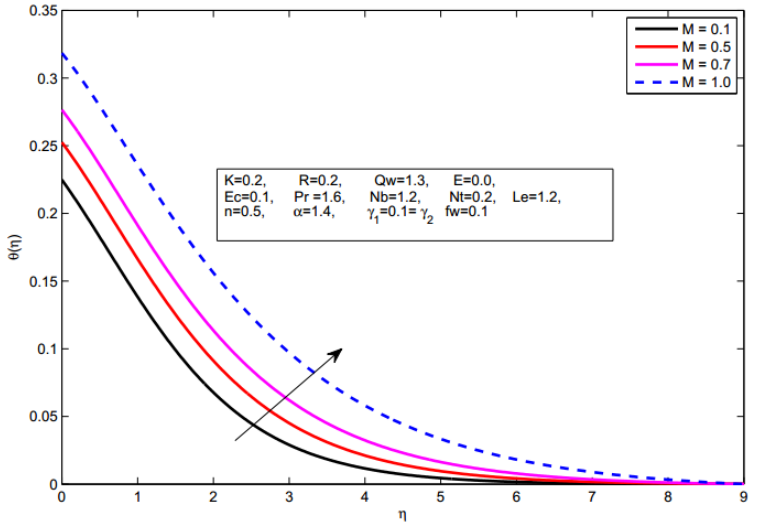

Figure 4.7: Impact of M on the unitless energy $\theta(\eta)$

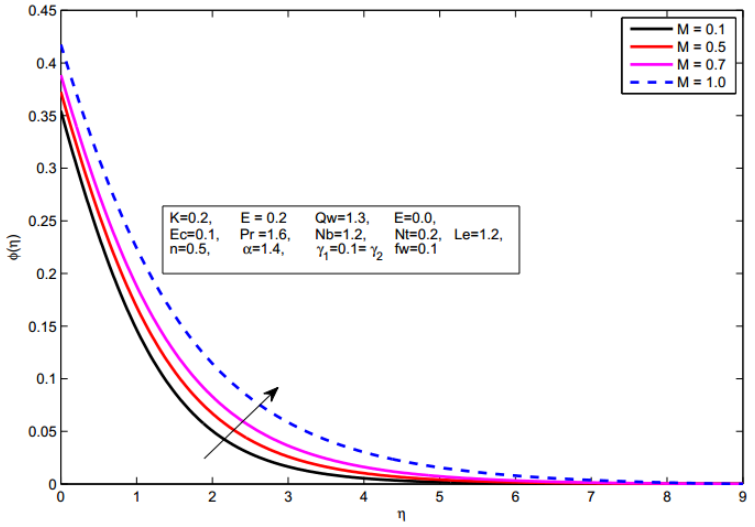

Figure 4.8: Impact of M on the unitless concentration $\phi(\eta)$

4.5.4 Impact of material parameter on the unitless micro-rotation profile and unitless velocity profile

Figures 4.9 and 4.10 show the influences of material parameter K on the microrotation profile $h(\eta)$ and velocity profile $f'(\eta)$ respectively.By increasing K, velocity field reduces in the lower half of the surface whereas it enhances in the upper half. Velocity reduces initially with the growing values of material parameter K. However for $\eta > 2.2$ there is an increase in the microrotation profile and for $\eta > 0.6$ there is an increase in the velocity profile.

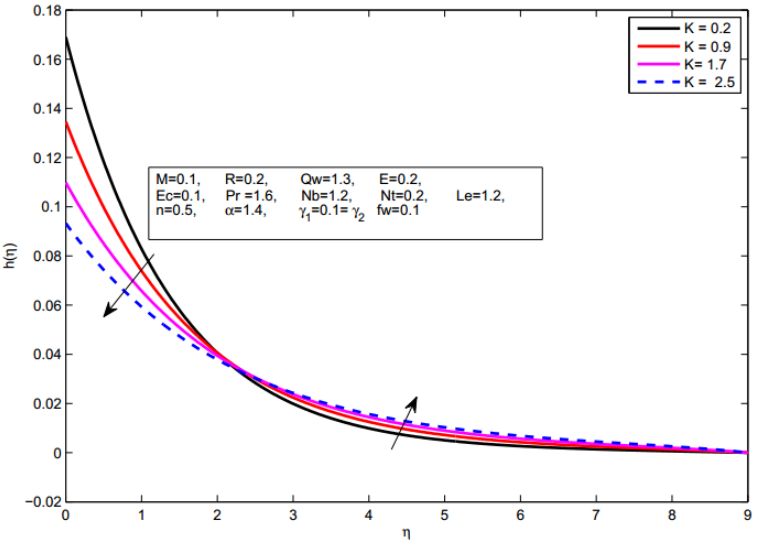

Figure 4.9: Impact of K on the unitless microrotation $h(\eta)$

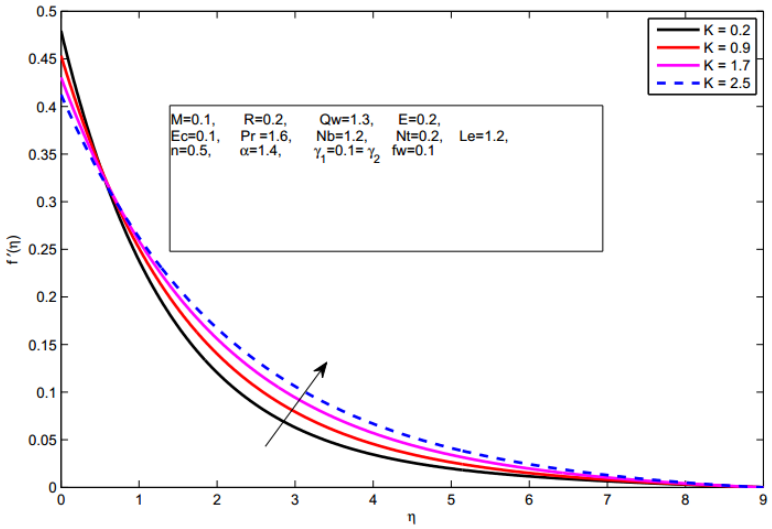

Figure 4.10: Impact of K on the unitless velocity $f'(\eta)$

4.5.5 Impact of Lewis number on the unitless concentration profile

Fig 4.11 show the influences of Lewis number Le on the concentration profile $\phi(\eta)$. The concentration profile is falls when we increase the values of Lewis number Le.

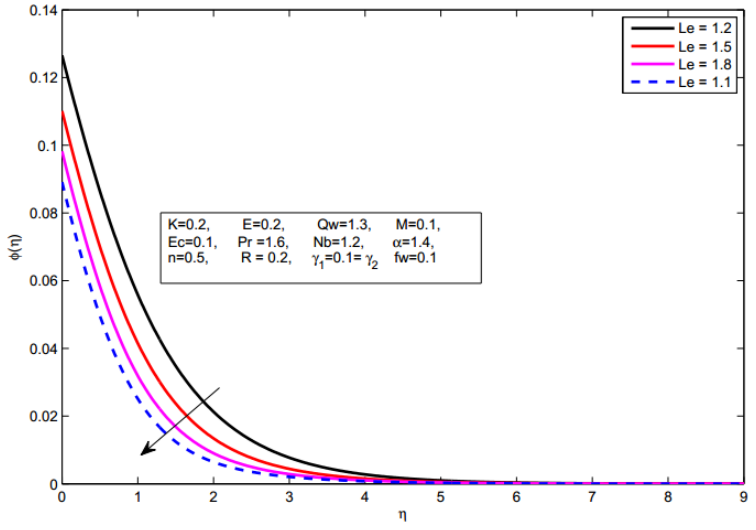

Figure 4.11: Impact of Le on the unitless velocity $\phi(\eta)$

4.5.6 Impact of thermal radiation parameter on unitless energy profile

Both the energy profile $\theta(\eta)$ and thermal boundary layer thickens are mounting function of heat rays parameter R. It is noticed as by increase in R results in increased thermal boundary layer.

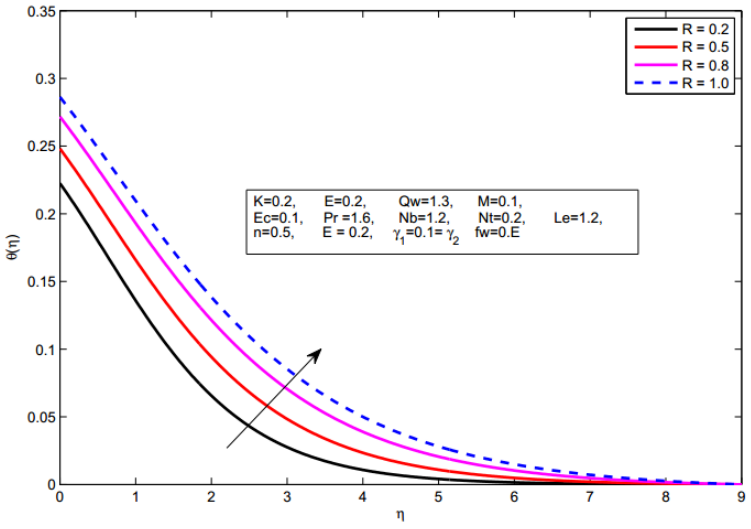

Figure 4.12: Impact of R on the unitless energy $\theta(\eta)$

4.5.7 Impact of Thermophoresis parameter on unitless energy profile and unitless concentration profile

Figure 4.13 and Figure 4.14 show the impact of Nt on the temperature profile $\theta(\eta)$ and concentration profile $\phi(\eta)$. Thermophoresis is a component that drives small materials away from hot layer to the cooler end, owing to the fact that both temperature profile $\theta(\eta)$ and concentration profiles $\phi(\eta)$ are growing function of thermophoretic parameter Nt.

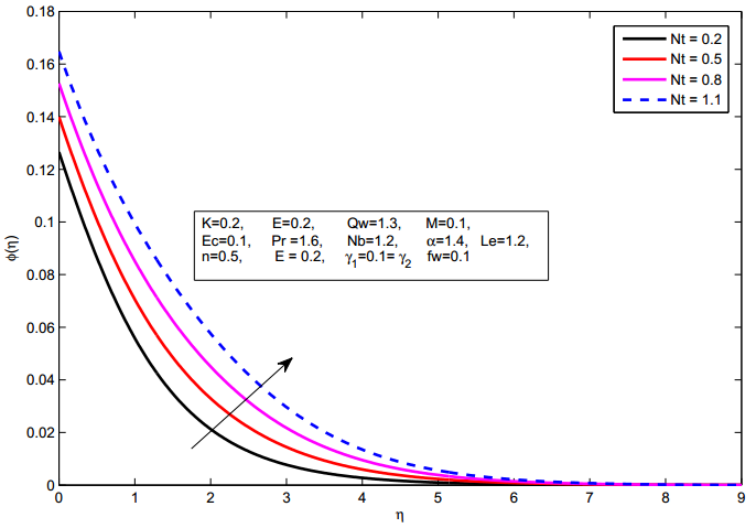

Figure 4.13: Impact of Nt on the unitless concentration $\phi(\eta)$

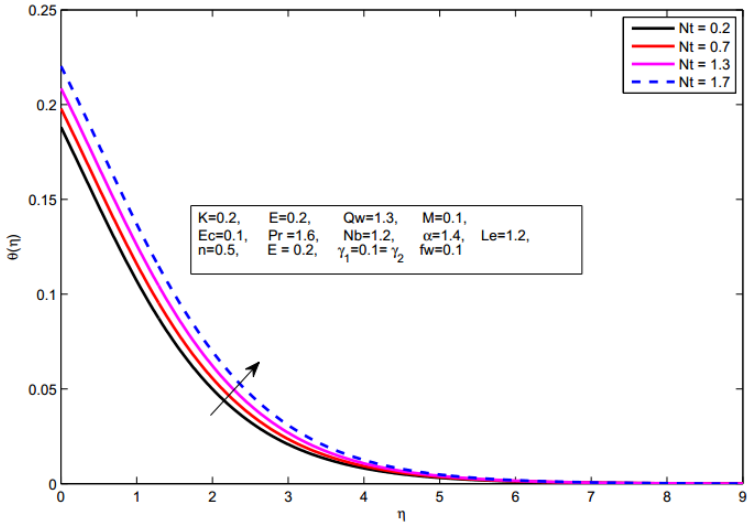

Figure 4.14: Impact of Nt on the unitless energy $\theta(\eta)$

4.5.8 Impact of Prandtl number on unitless temperature profile and unitless concentration profile

Figure 4.15 and Figure 4.16 presents that an elevation in Prandtl number Pr shows a redaction in the temperature profile $\theta(\eta)$ and concentration profile $\phi(\eta)$. Obviously, greater Prandtl number Pr has weaker thermal diffusivity due to which low range temperature is seen in Fig. 4.17 and Fig. 4.18. This indicates resection in energy exchange ability and finally it causes an reduction in thermal boundary surface.

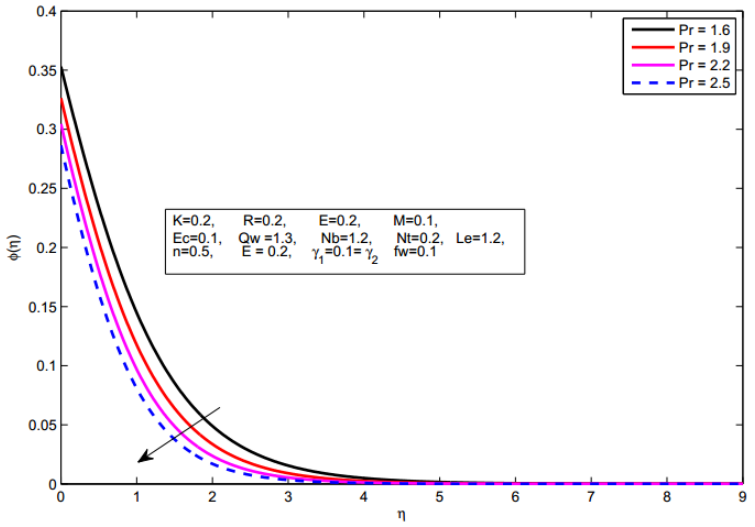

Figure 4.15: Impact of Pr on the unitless concentration $\phi(\eta)$

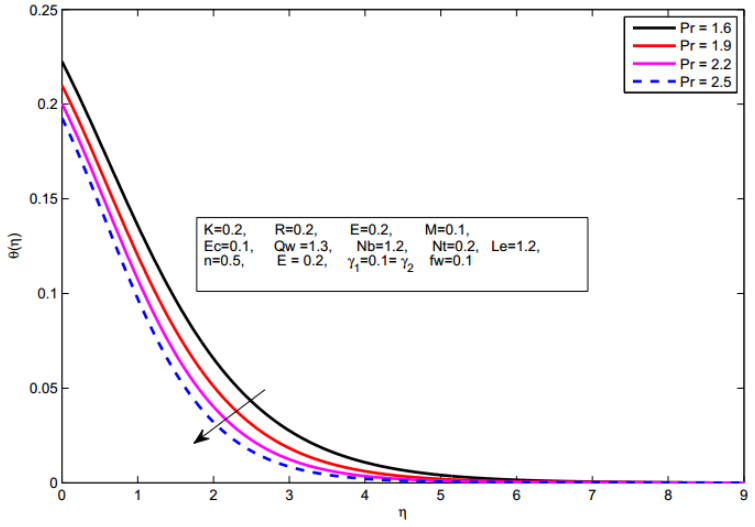

Figure 4.16: Impact of Pr on the unitless energy $\theta(\eta)$

4.5.9 Impact of temperature ratio parameter on unitless energy profile and unitless concentration profile

Figure 4.17 represents the impact of the temperature ratio parameter Qw on energy profile. The increase in temperature ratio parameter Qw increases the thermal condition of the fluid, resulting in an expansion in energy profiles.

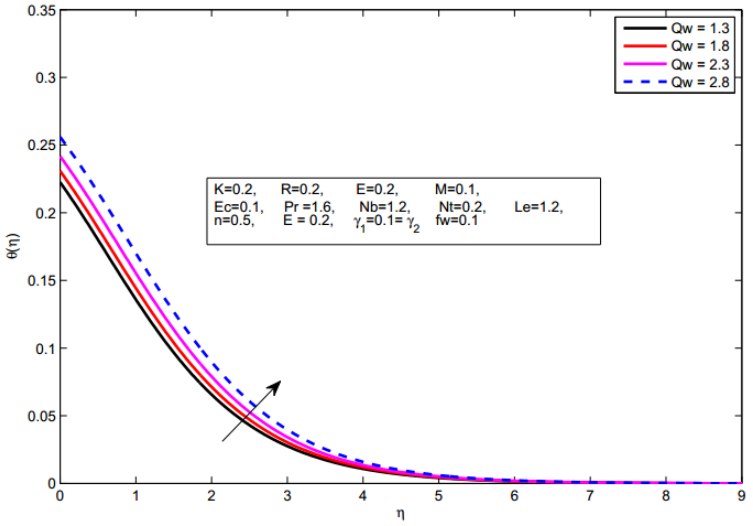

Figure 4.17: Impact of Qw on the unitless energy $\theta(\eta)$

4.5.10 Skin-friction coefficient, Nusselt number and Shewood number

Both the physical parameters C_f , Nu_x and Sh_x are of great interest to engineers. C_f is the one which examines the viscus stress acting on the surface of the plate.

Parameters					$1/2C_{fx}Re_x^{1/2}$		$NuRe_x{}^{-1/2}$		$ShRe_x^{-1/2}$	
K	M	n	fw	α	Shooting	bvp4c	Shooting	bvp4c	Shooting	bvp4c
0.2					-0.37183	-0.37183	0.10528	0.10671	0.08734	0.08734
0.3					-0.37483	-0.37483	0.10525	0.10669	0.08735	0.08735
0.4					-0.37769	-0.37769	0.10522	0.10666	0.08736	0.08736
0.2	0.2				-0.37093	-0.37093	0.10553	0.10692	0.08743	0.08743
	0.3				-0.37052	-0.37052	0.10576	0.10711	0.08752	0.08752
	0.4				-0.37112	-0.37112	0.10592	0.10725	0.08757	0.08757
	0.1	0.6			-0.37073	-0.37073	0.10522	0.10666	0.08734	0.08734
		0.7			-0.36959	-0.36959	0.10516	0.10661	0.08733	0.08733
		0.8			-0.36842	-0.36842	0.10510	0.10655	0.08733	0.08733
		0.5	0.2		-0.38154	-0.38154	0.11036	0.10914	0.08888	0.08888
			0.3		-0.39134	-0.39134	0.11519	0.11114	0.09014	0.09014
			0.4		-0.40120	-0.40120	0.11984	0.11281	0.09119	0.09119
			0.1	1.5	-0.35621	-0.35621	0.10514	0.10660	0.08720	0.08720
				1.6	-0.34191	-0.34191	0.10500	0.10649	0.08707	0.08707
				1.7	-0.33785	-0.32877	0.10496	0.10638	0.08704	0.08695

Table 4.1: Numerical results of $1/2C_{fx}Re_x^{1/2}$, $Nu/Re_x^{1/2}$ and $Sh_xRe_x^{-1/2}$ for different values of R, Qw, Pr, Ec and Nb

Parameters					$NuRe_x{}^{-1/2}$		$ShRe_x^{-1/2}$	
R	Qw	Pr	Ec	Nb	Shooting	bvp4c	Shooting	bvp4c
0.3					0.11587	0.11733	0.08736	0.08734
0.4					0.12622	0.12938	0.08739	0.08734
0.5					0.13633	0.14143	0.08741	0.08734
0.2	1.4				0.10596	0.10614	0.08734	0.08734
	1.5				0.10665	0.10701	0.08735	0.08734
	1.6				0.10735	0.10791	0.08735	0.08734
	1.3	1.7			0.10597	0.10528	0.08780	0.08734
		1.8			0.10659	0.10528	0.08821	0.08734
		1.9	0.2		0.10716	0.10528	0.08860	0.08734
			0.3		0.10312	0.10528	0.08741	0.08734
			0.4		0.10097	0.10528	0.08747	0.08734
			0.1	1.3	0.09882	0.10528	0.08754	0.08734
				1.4	0.10510	0.10528	0.08742	0.08734
				1.5	0.10493	0.10528	0.08748	0.08734

Table 4.2: Numerical results of $Nu/Re_x^{1/2}$ and $Sh_xRe_x^{-1/2}$ for different values of R, Qw, Pr, Ec and Nb

Parameters				$NuRe_x{}^{-1/2}$		$ShRe_x^{-1/2}$	
Nt	Le	γ_1	γ_2	Shooting	bvp4c	Shooting	bvp4c
0.3				0.10503	0.10650	0.08689	0.08689
0.4				0.10478	0.10629	0.08644	0.08644
0.5				0.10453	0.10607	0.08600	0.08600
0.2	1.3			0.10533	0.10675	0.08795	0.08795
	1.4			0.10538	0.10679	0.08850	0.08850
	1.5			0.10543	0.10683	0.08898	0.08898
	1.2	0.2		0.17775	0.18498	0.08669	0.08669
		0.3		0.22928	0.24361	0.08624	0.08624
		0.4		0.26719	0.28861	0.08592	0.08592
		0.1	0.2	0.10358	0.10526	0.15643	0.15643
			0.3	0.10210	0.10401	0.21246	0.21246
			0.4	0.10082	0.10291	0.25880	0.25880

Table 4.3: Numerical results of $Nu/Re_x^{1/2}$ and $Sh_xRe_x^{-1/2}$ for different values of Nt, Le, γ_1 and γ_2

In Table 4.1, 4.2 and 4.3 the numerical analysis of C_f, S_h and Nu_x on different physical parameters is displayed. We compare the results obtained by Shooting method with Matlab bvp4c code and found both to be in excellent agreement. It is observed, the increase in Hartman number M and Suction/Injection velocity f_w enhance the local skin-friction coefficient, local Nuselt number and Sherwood number. Moreover, the local Nusselt number and Sherwood number falls by enlarging the Eckert number Ec, and Thermophoresis parameter Nt. Whereas local skin-friction coefficient, Nusselt number, Sherwood number shows a decreasing behavior for Buoyancy ratio parameter n and slip parameter α. The local Nusselt number and Sherwood number mounts when enlarging Radiation parameter R, Temperature ratio parameter Qw, Prandtl number Pr and Lewis number Le.

4.6 Summary

In this chapter, the flow of micropoler fluid past a penetrable stretching sheet in the presence of Joule heating and magneto MHD with moving fluid boundary conditions, is presented. The dimensionless velocity, dimensionless energy, dimensionless concentration and dimensionless micro-rotation are analyzed and presented in the form of graphs and tables. We present the Nusselt number, Sherwood number and local skin-friction in the tabular form for various number of the distinctive parameters. From the above discussion, we can make the following conclusions.

- Higher values of M yields an increment in the energy profile and Concentration profile whereas an opposite effect has noticed for the velocity profile.
- An increase in α results in enhanced energy as well as concentration profile.
- Energy profile θ increases by enlarging Ec.
- The energy profile θ increase and concentration profile ϕ reduces with an increase in Nb.
- The energy profile θ and concentration profile ϕ increases with an increase in Nt.
- For larger values of Pr energy profile θ and concentration profile ϕ shows decreasing behavior.
- The velocity profile f' increases by enlarging K.
- The Energy profile increases by enlarging R and Qw.
- The concentration profile ϕ reduces with an increase in Le.

Chapter 5

Conclusion

In this thesis, we discuss the partial slip effects of magneto-micropolar nanofluid movement and heat exchange past a convectively heated sheet along with nonlinear thermal radiation and resistive losses. The reduced system of ODEs after applying a proper similarity transform are solved numerically. Numerical solution of these modeled ODEs are acquired by using shooting method. A numerical comparison has displayed for various physical parameters affecting flow and heat transfer and found to be in excellent agreement with Matlab bvp4c code. Significance of different physical parameters under discussion on dimensionless velocity, microrotation, energy and concentration profile are depicted spectrally for the effect of appropriate parameters. In general, It is obvious, the inflated in Hartman number M and Suction/Injection velocity fw enhance the local skin-friction coefficient, local Nusselt number and Sherwood number. For increasing values of Thermal Biot number γ_1 local Nusselt number is increase but Sherwoof number is decrease, But on the other hand for increasing values of Concentration Biot number γ_2 the local Nusselt number decrease and Sherwood number mounts.

Bibliography

[1] A. Ahmad, S. Afzal, and S. Asghar. Semi-inverse solution for transient MHD flow of a second grade fluid past a stretching surface. *American Institute of Physics*, 10:127140, 2015.

[2] M. Ramzan and M. Bilal. Time dependent MHD nano-second grade fluid flow induced by permeable vertical sheet with mixed convection and thermal radiation. *Public Library of Science*, 64:e0124929, 2015.

[3] R. Ellahi. The effects of MHD and temperature dependent viscosity on the flow of non - Newtonian nanofluid in a pipe. *Applied Mathematical Modelling*, 3:1451–1467, 2013.

[4] M. Govindaraju, N. V. Ganesh, B. Ganga, and A. A. Hakeem. Entropy generation analysis of magnetohydrodynamic flow of a nanofluid over a stretching sheet. *Egyptian Mathematical Society*, 2:429–434, 2015.

[5] M. Sheikholeslami, H. Hatami, and D. D. Ganji. Nanofluid flow and heat transfer in a rotating system in the presence of a magnetic field. *Journal of Molecular Liquids*, 190:112–120, 2014.

[6] Y. Lin, L. Zheng, X. Zhang, L. Ma, and G. Chen. MHD pseudo-plastic nanofluid unsteady flow and heat transfer in a finite thin film over stretching surface with internal heat generation. *International Journal of Heat and Mass Transfer*, 84:903–911, 2015.

[7] T. Hayat, T. Muhammad, S. A. Shehzad, G. Q. Chen, and I. A. Abbas. Interaction of magnetic field in flow of Maxwell nanofluid with convective effect. *Journal of Magnetism and Magnetic Materials*, 389:48–55, 2016.

[8] A. Ahmad and S. Asghar. Flow of a second grade fluid over a sheet stretching with arbitrary velocities subject to a transverse magnetic field. *Applied Mathematics Letters*, 24:1905–1909, 2011.

[9] T. Hayat, A. Aziz, T. Muhammad, and B. Ahmad. On magnetohydrodynamic flow of second grade nanofluid over a nonlinear stretching sheet. *Journal of Magnetism and Magnetic Materials*, 408:99–106, 2016.

[10] P. D. Ariel. On computation of MHD flow near a rotating disk. *Math. Mech. Zeitschrift for Angewandte Mathematik and Mechanik*, 82:235–246, 2002.

[11] R. Ahmad, M. Mustafa, T. Hayat, and A. Alsaedi. Numerical study of MHD nanofluid flow and heat transfer past a bidirectional exponentially stretching sheet. *Magnetism and Magnetic Materials*, 407:69–74, 2016.

[12] M. Sheikholeslami, T. Hayat, and A. Alsaedi. A note on a certain boundary-layer equation. *International Journal of Heat and Mass Transfer*, 96:513–524, 2016.

[13] M. Sheikholeslam, K. Vajravelu, and M. M. Rashidi. Forced convection heat transfer in a semi annulus under the influence of a variable magnetic field. *International Journal of Heat and Mass Transfer*, 92:339–348, 2016.

[14] P. M. Krishna, N. Sandeep, and V. Sugunamma. Effects of radiation and chemical reaction on MHD convective flow over a permeable stretching surface with suction and heat generation. *Web Journey Science and Technology*, 12:831–847, 2015.

[15] Z. Abbas, M. Naveed, and M. Sajid. Hydromagnetic slip flow of nanofluid over a curved stretching surface with heat generation and thermal radiation. *Journal of Molecular Liquids*, 215:756–762, 2016.

[16] R. U. Haq, S. Nadeem, Z. H. Khan, and N. S. Akbar. Thermal radiation and slip effects on MHD stagnation point flow of nanofluid over a stretching sheet. *Physics E*, 65:27–23, 2015.

[17] M. Sheikholeslami, D. D. Ganji, M. Y. Javed, and R. Ellahi. Effect of thermal radiation on magnetohydrodynamics nanofluid flow and heat transfer by means of two phase model. *Journal of Magnetism and Magnetic Materials*, 374:36–43, 2015.

[18] E. M. Abo-Eldahab and M. E. Elbarbary. Hall current effect on magnetohydrodynamic free-convection flow past a semiinfinite vertical plate with mass transfer. *International Journal of Engineering Science*, 60:1641–1652, 2001.

[19] E. M. Abo-Eldahab and M. A. Aziz. Hall current and Ohmic heating effects on mixed convection boundary layer flow of a micropolar fluid from a rotating cone with power-law fluid at a stretching surface. *International Communications in Heat and Mass Transfer*, 31:751–762, 2004.

[20] A. M. Salem and M. A. El-Aziz. Effects of Hall current and chemical reaction on hydromagnetic flow of a stretching vertical surface with internal heat generation/absorption. *Applied Mathematical Modelling*, 55:1236–1254, 2008.

[21] A. C. Eringen. Theory of micropolar fluids. *Journal of Applied Mathematics*, 16:1–18, 1966.

[22] S. Nadeem, S. Masood, R. Mehmood, and M. A. Sadiq. Optimal and numerical solutions for an MHD micropolar nanofluid between rotating horizontal parallel plates. *Public Library of Science*, 10 (6):e0124016, 2016.

[23] M. Fakoura, A. Vahabzadeh, D. D. Ganji, and M. Hatami. Analytical study of micropolar fluid flow and heat transfer in a channel with permeable walls. *Journal of Molecular Liquids*, 204:198–204, 2015.

[24] T. Hayat, S. A. Shehzad, and M. Qasim. Mixed convection flow of a micropolar fluid with radiation and chemical reaction. *International Journal for Numerical Methods in Fluids*, 67:1418–1436, 2011.

[25] S. U. S. Choi. Enhancing thermal conductivity of fluids with nanoparticles. *Fluids Engineering Division Executive Committee*, 66:99–105, 1995.

[26] O. D. Makinde and A. Aziz. Boundary layer flow of a nanofluid past a stretching sheet with a convective boundary condition. *International Journal of Thermal Sciences*, 50:1326, 2011.

[27] Y. Lin, L. Zheng, X. Zhang, L. Ma, and G. Chen. MHD pseudo-plastic nanofluid unsteady flow and heat transfer in a finite thin film over stretching surface with internal heat generation. *International Journal of Heat and Mass Transfer*, 84:903–911, 2015.

[28] M. Sheikholeslami, M. M. Rashidi, T. Hayat, and D. D. Ganji. Free convection of magnetic nanofluid considering MHD viscosity effect. *Journal of Molecular Liquids.*, 218:393–399, 2016.

[29] W. A. Khan and I. Pop. Boundary layer of nanofluid past a stretching sheet. *International Journal of Heat and Mass Transfer*, 53:2477–2483, 2010.

[30] D. Pal, G . Mandal, and K. Vajravelu. MHD convection-dissipation heat transfer over a non - linear stretching and shrinking sheet in nanofluids with thermal radiation. *International Journal of Heat and Mass Transfer*, 65:480–490, 2013.

[31] M. M. Rashidi, S. Abelman, and N. F. Mehr. Entropy generation in steady MHD flow due to a rotating porous disk in a nanofluid. *International Journal of Heat and Mass Transfer*, 62:515–525, 2013.

[32] M. Sheikholeslami, R. Ellahi, H. R. Ashorynejad, G. Domairry, and T. Hayat. Effects of heat transfer in flow of nanofluids over a permeable stretching wall in a porous medium. *Applied Mathematical Modelling*, 11:486–496, 2014.

[33] A. Zeeshan, M. Baig, R. Ellahi, and T. Hayat . Flow of viscous nanofluid between the concentric cylinders. *Applied Mathematics and Computation*, 11:646–654, 2014.

[34] M. Sheikholeslami and S. Abelman. Two-phase simulation of nanofluid flow and heat transfer in an annulus in the presence of an axial magnetic field.

Institute of Electrical and Electronics Engineers Transactions on Nanotechnology, 14:561–569, 2015.

[35] C. Zhang, L. Zheng, X. Zhang, and G. Chen. MHD flow and radiation heat transfer of nanofluids in porous media with variable surface heat flux and chemical reaction. *Applied Mathematical Modellingl*, 39:165–181, 2015.

[36] M. Ramzan, M. Farooq, T. Hayat, and J. D. Chung. Radiative and Joule heating effects in the MHD flow of a micropolar fluid with partial slip and convective boundary condition. *Molecular Liquids*, 10.1016:05–091, 2016.

[37] R. K. Bansal. Fluid mechanics and hydraulic machines. *Laxmi Publications (P) Ltd*, 21:3–163, 1983.

[38] R. W. Fox, A. T. McDonald, and P. J. Pritchard. Introduction to fluid mechanics. *Wiley*, 6:16–340, 2003.

[39] V. K. Garg. Applied computational fluid dynamics. *C. R. C. Press*, 116:1–6, 1998.

[40] K. Vafai. Handbook of porous media. *C. R. C Press*, 2:141–377, 2005.